Research Department

Technical Report No. 68

Implementation of a third generation ocean wave model at the European Centre for Medium-Range Weather Forecasts

H. Günther[1], P. Lionello[2], P.A.E.M. Janssen[3], L. Bertotti[2], C. Brüning[4], J.C. Carretero[5], L. Cavaleri[2], A. Guillaume[6], B. Hansen[4], S. Hasselmann[4], K. Hasselmann[4], M. de las Heras[3], A. Hollingsworth, M. Holt[7], J.M. Lefevre[6], R. Portz[4]

European Communities Contract No. SC1-0013-C(GDF)(SC1000013)

1 *On leave from GKSS, Geesthacht, Germany*
2 *Presently at ISDGM-CNR, Venice, Italy*
3 *KNMI, de Bilt, The Netherlands and ECMWF*
4 *MPIfM, Hamburg, Germany*
5 *MOPU/PCM, Madrid, Spain*
6 *DMN, Paris, France*
7 *UKMO, Bracknell, UK*

August 1992

Abstract

Interest in accurate modelling of the ocean wave conditions has steadily grown in the past decade. Besides the traditional hindcast and forecast applications (e.g. guidance of off-shore marine operations) important new applications have emerged. As examples we mention the use of wave information for the interpretation of satellite sensors and the modelling of fluxes through the air-sea interface. On the other hand, the use of satellite data in wave data assimilation provides the potential to improve results on wave forecasting.

The development of modern wave modelling capabilities in conjunction with extended wind and wave assimilation techniques, therefore, forms a key element in the longer term European programs.

The aim of the present two-year project was

1) to implement the existing third generation model, jointly developed by the WAM group (*WAMDI*, 1988) into the operational environment at the European Centre for Medium-Range Weather Forecasts (ECMWF)

2) to develop a data assimilation system to utilise the wealth of ERS-1 satellite data and

3) to investigate coupling between wave and atmospheric models.

The following conclusions resulted from the project:

- The third generation WAM wave model was extensively tested and technically and physically improved. The final cycle 4.0 version has become the standard model of the WAM group. It has been implemented operationally at ECMWF together with the required archiving and diagnostic software. The distribution of 10-day wave forecast products will start in 1992 as part of ECMWF's optional wave program.

- The cycle 4.0 of the WAM model is organised as a subroutine version. It needs less computer resources than previous cycles. New options, such as nesting, depth and current refraction have been added.

- New input and dissipation source functions have been developed and introduced into cycle 4.0. The new physics takes into account that the wind and, therefore, the momentum flux through the sea surface is sea-state dependent. Tests with atmospheric and surge models coupled with the WAM model have demonstrated the benefits.

- The model was extensively verified against buoy and satellite altimeter measurements. Cycle 4.0 of the wave model forced by T213 wind fields of ECMWF agrees remarkably well with buoy and satellite wave height data.

- A wave and wind data assimilation system based on Optimal Interpolation was further

developed and combined with the wave model. By careful tuning we obtained a more prolonged impact of the measured data, and better wave forecasts were produced.

- The combined wave prediction and assimilation system is ready for operational use. It was successfully applied in a quasi-operational mode during the calibration/validation phase of ERS-1 to monitor the performance of the satellites' altimeter. Due to the delayed launch of ERS-1 impact studies with calibrated ERS-1 data had to be postponed until mid 1992.

Overall, it may be concluded that all goals of the operations project have been reached.

At its 34th session (June 1991) the Council of ECMWF approved the implementation of an Optional Project for Prediction of Ocean Waves with a starting date on 1 January 1992 and with operational implementation in the middle of 1992. The Project was supported by 13 Member States.

CONTENTS

1. INTRODUCTION

In recent years the demand for accurate modelling of ocean wave conditions has steadily grown. Besides the traditional hindcast and forecast applications to generate climatologies and extreme value statistics, and guidance for off-shore marine operations, new important applications have arisen. The use of wave information for the interpretation of satellite sensors and the modelling of fluxes through the atmosphere ocean boundary are two main areas.

The use of satellite data in wave data assimilation systems provides the opportunity to improve the forecast results and forecast range for wave models.

Therefore the development of modern wave modelling capabilities in conjunction with extended wind and wave data assimilation techniques forms a key element in the longer term European programs.

The aims of this two year project was to implement the existing third generation wave model, jointly developed by the WAM group (WAMDI 1988) into the operational environment at the European Centre for Medium Range Weather Forecasts (ECMWF), to develop a data assimilation system, and to investigate a coupling between wave and atmospheric models.

Results presented in this report were achieved by close cooperation in the WAM (Wave modelling) Group. The main part of the work was done at ECMWF, supported by visiting scientists from the other institutes participating in this special project:

- Koninklijk Nederlands Meteorologisch Instituut (KNMI), De Bilt, The Netherlands
- GKSS-Forschungzentrum (GKSS), Geesthacht, Germany
- Max-Planck-Institut für Meteorologie (MPIfM), Hamburg, Germany
- Meteorological Office (UKMO), Bracknell, England
- Meteorologie National (DMN), Paris, France
- Instituto per lo Studio della Dinamica della Grandi Masse del Consiglio Nazionale delle Richerche (ISDGM), Venezia, Italy
- Ministeros de Obras Publicas y Urbanismo, Programa de Clima Maritimo y Banco de Datos Oceanograficos (MOPU), Madrid, Spain.

The project was coordinated by a technical advisory board, formed by one representative of the participating institutes, in bi-annual meetings, chaired by G. Komen (KNMI).

This report is organized in three main chapters to present the results achieved for each of the goals given above. In particular Chapter 2 summarizes the work done for the operational implementation. This includes the model development, code optimization, the archiving and verification. The results of comparisons with GEOSAT and ERS-1 radar altimeter measurements, buoy data and the wave model of the UK Meteorological Office are shown. Model experiments to check the forecast performance and the effect of higher resolution will be summarized.

Chapter 3 outlines the work which has been carried out to develop and implement a wave data assimilation system. This includes the organisation of data flow and quality control. A number of tests with SEASAT, GEOSAT, and ERS-1 are discussed.

Chapter 4 presents the developments towards a coupled wave atmospheric model, which led to a new formulation of the wave model input and dissipation source functions.

The principal results of this project and some recommendations for further work are outlined at the end of this report.

1.1 Establishment of a Project at ECMWF for prediction of ocean waves

At its 30th session (May 1989) the Council of ECMWF agreed to the principle of 'Optional Projects', in which some Member States could decide not to participate. A procedure for the establishment of such projects was agreed.

At its 34th session (June 1991) the Council of ECMWF approved the implementation of an Optional Project for Prediction of Ocean Waves with a starting date on 1 January 1992 and with operational implementation in the middle of 1992. The Project was supported by 13 Member States.

2. WAVE MODEL DEVELOPMENT

The basis of the development of an operational implementation of a wave model at ECMWF was the cycle 2.0 of the third generation WAM model. For a detailed description see WAMDI (1988). This version has been used at ECMWF for validation against buoy measurements over a period of one year (*Zambresky*, 1989).

The main efforts were concentrated on technical developments to enable the wave model to run as a sub-process of the atmospheric model, and on model performance studies, such as comparisons with measurements and other wave models.

2.1 From Cycle 2.0 to Cycle 4.0

The technical development of the model code was done in two major steps. The first aim was to combine and reorganise the stand-alone programs of cycle 2.0 into cycle 3.0, which is a subroutine version which can run as a sub-process of the atmospheric model. A subroutine version is the necessary condition to prepare the models for a two way coupling (cf. *Weber et al.* 1991). In addition this code reorganisation provided the opportunity to improve the programs with respect to computer time and memory requirement, plus internal model documentation, as required for an operational forecast.

This new model structure achieves savings of about 25% as shown in Table 1, which compares the computer requirements of cycle 2.0 and cycle 3.0 on a CRAY XMP (single processor). The model runs were done on a global 3-degree latitude longitude grid; the wave spectra were represented by 25 frequencies and 12 directions.

	Cycle 2.0	Cycle 3.0	Change
CPU (Minutes)	5:06	3:59	-22%
Memory (MWords)	1.67	1.35	-19%
Disk moves (MWords)	315	204	-35%
Temp. Data (MWords)	7.4	5.4	-27%
Restart files (MBytes)	23.45	16.11	-31%
UNITS	441	327	-26%

Table 1: Performance on Cray XMP of Cycle 2.0 and 3.0

Parallel to the code reorganisation at ECMWF a number of new features had been developed by the WAM group,especially at the MPIfM. It was decided to combine the different model versions to a common

Cycle 4.0 based on the structure of ECMWF's subroutine version. In particular the model was extended to allow nested grids, current and depth refraction. The propagation algorithm was changed to a flux scheme and a number of errors discovered during the reorganisation have been corrected.

In addition to these technical improvements, the physics of the model has been changed. This was done with respect to the atmospheric input source function and the dissipation source function to take into account the dependence of the growth rate on the wave stress. A description of the 'new' physics is presented in chapter 4 and in *Janssen* (1991). Additional technical information may be obtained from the wave model user guide of cycle 4.0 (*Günther et al.*, 1992).

The computer performance relative to cycle 3.0 on the Cray YMP (single processor) is given in Table 2. The increase in the cpu-time by 14% is related to the new physics, the corrections to the non-linear interactions and additional output. The savings in data transfer and file length was achieved by optimizing model set-up parameters, e.g. the model block length.

	Cycle 3.0	Cycle 4.0	Change
CPU (Minutes)	2:37	2:59	+14%
Memory (MWords)	4.77	4.12	-14%
Data Transfer (MWords)	205	117	-43%
Restart files (MBytes)	16.11	9.03	-44%

Table 2: Performance on Cray YMP of Cycle 3.0 and 4.0

This version of cycle 4.0 is used for daily test runs at ECMWF since November 1991 and runs under full control of the Centre's operational system. This set-up will become operational as an ECMWF Optional Project in 1992. The model job stream is given in Appendix 1.

2.2 Archiving and diagnostics software

Besides the operational execution of the model itself it is essential to archive the results of the analysis and forecast in a format, which allows easy access and international distribution. Furthermore a number of diagnostics programs are necessary to monitor the model results. A postprocessing job has been included in the daily job stream controlled by ECMWF's operational system to pack the global model fields of significant wave heights, mean wave directions, mean wave periods and wave peak periods into the WMO code FM92 GRIB and to store this data into ECMWF's meteorological archive MARS.

To monitor the daily model results global maps for the wave analysis (Fig. 1) and forecast (Fig. 2) are plotted. Both plots show the wave heights and directions on December, 24th 1991. Fig. 1 is computed with analysed winds and Fig. 2 is a 24 hour prediction using the Centres forecast wind. Besides a small overprediction of the storm waves in the South Atlantic, the forecast agrees quite remarkably with the analysis.

Monthly global wave and wind statistics are generated by this postprocessing job (see Figs. 3 and 4). The climate data are saved in the mass storage ECFILE, since April 1990.

A second postprocessing job is daily executed to collocate model results with buoy measurements. The monthly collocation files are saved in ECFILE since September 1991. Results of this verification are shown in the next chapter.

Besides this operational postprocessing software many programs have been developed to access the different model output and to print or plot the data or to perform statistics. Examples are shown in the following chapters.

All software is adapted to the latest versions of ECMWF's libraries and are set-up to keep track of all changes in data format since 1987 when the first test runs were done.

2.3 Model validation

2.3.1 *Comparison with buoy data*

An extensive wave model (cycle 2.0) validation against buoy measurements over a period of one year was carried out by *Zambresky* (1989). Due to changes in ECMWF's computer, archive and plot system a complete redesign and programming of her analysis software was necessary.

One of the conclusions of L. Zambresky's validation was that the model predicts wave heights quite accurately. However, an underprediction of the wave height maxima was noted. The upper panel of Fig. 5 is taken out of her report and shows the wave heights comparison at buoy 46001 located in the Gulf of Alaska for January 1988. The lower panel of Fig. 5 shows a reanalysis of the data from the cycle 2.0 model run. Zambresky interpolated the model data to the buoy location. In the reanalysis however the model results from the nearest grid point were taken. An excellent agreement between model and measurements could be achieved. Because buoy 46001 is located within one 3 degree gridcell of the coast line, coastal effects like shadowing could be minimized by this method. The overall statistics are only marginally affected by this change in the collocation procedure, because extreme events do not occur so frequently and the new method does not affect the comparisons in the open ocean (see 2.4). Each

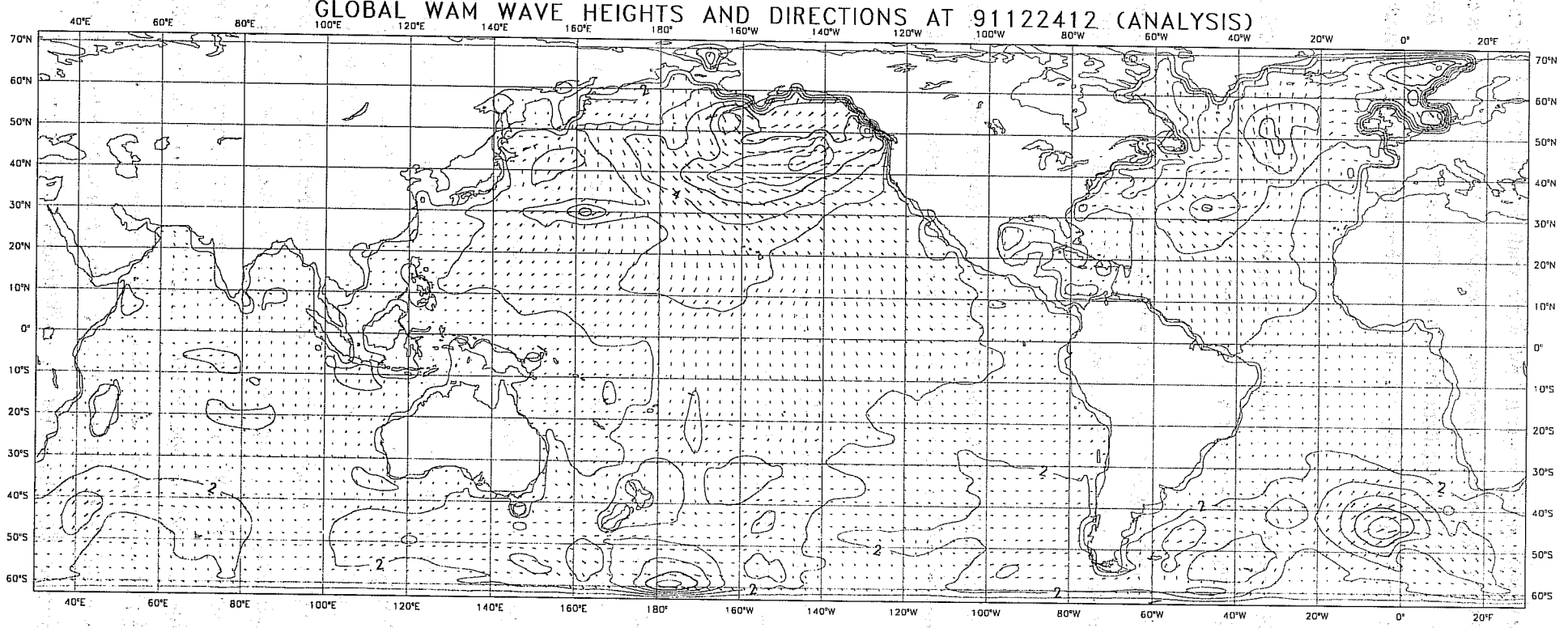

Fig. 1 Global map of significant wave height and direction for 24 December 1991 12:00 UT from the WAM model (cycle 4.0) forced by ECMWF's T213 analysed winds.

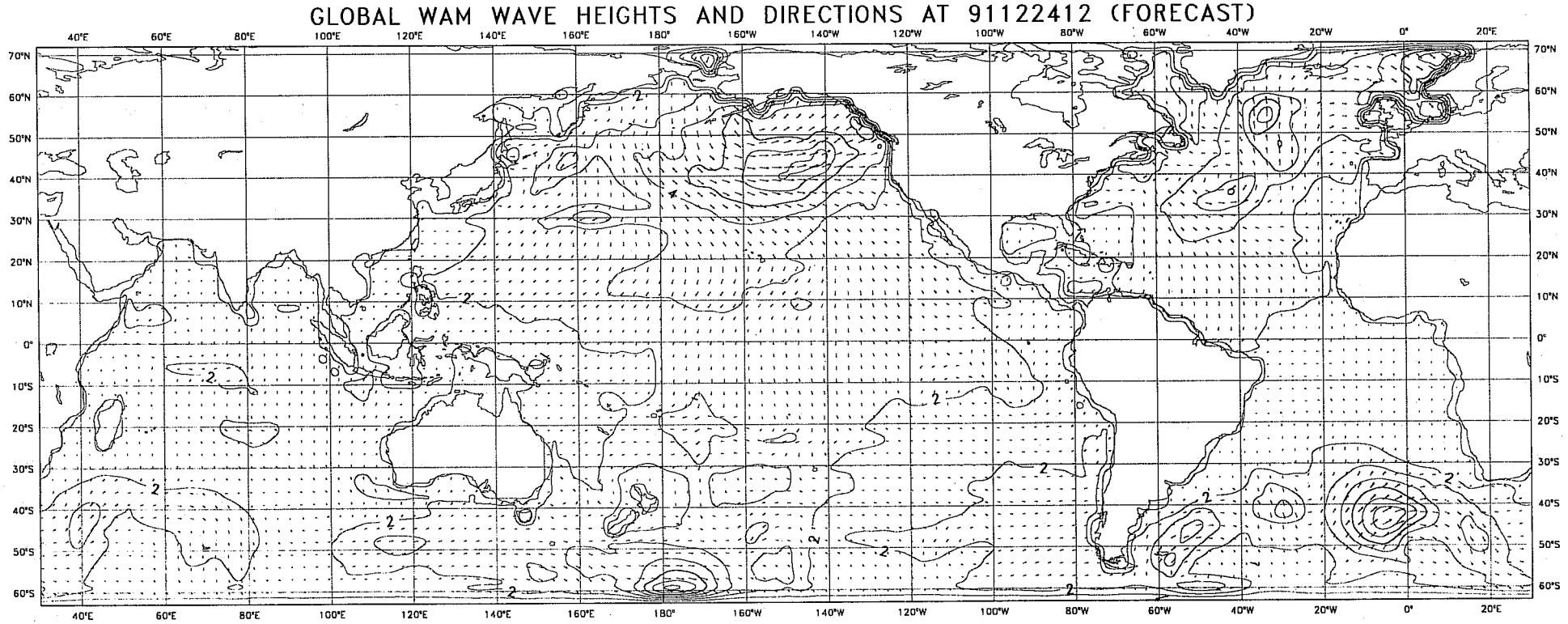

Fig. 2 Same as Fig. 1 but 24h forecast.

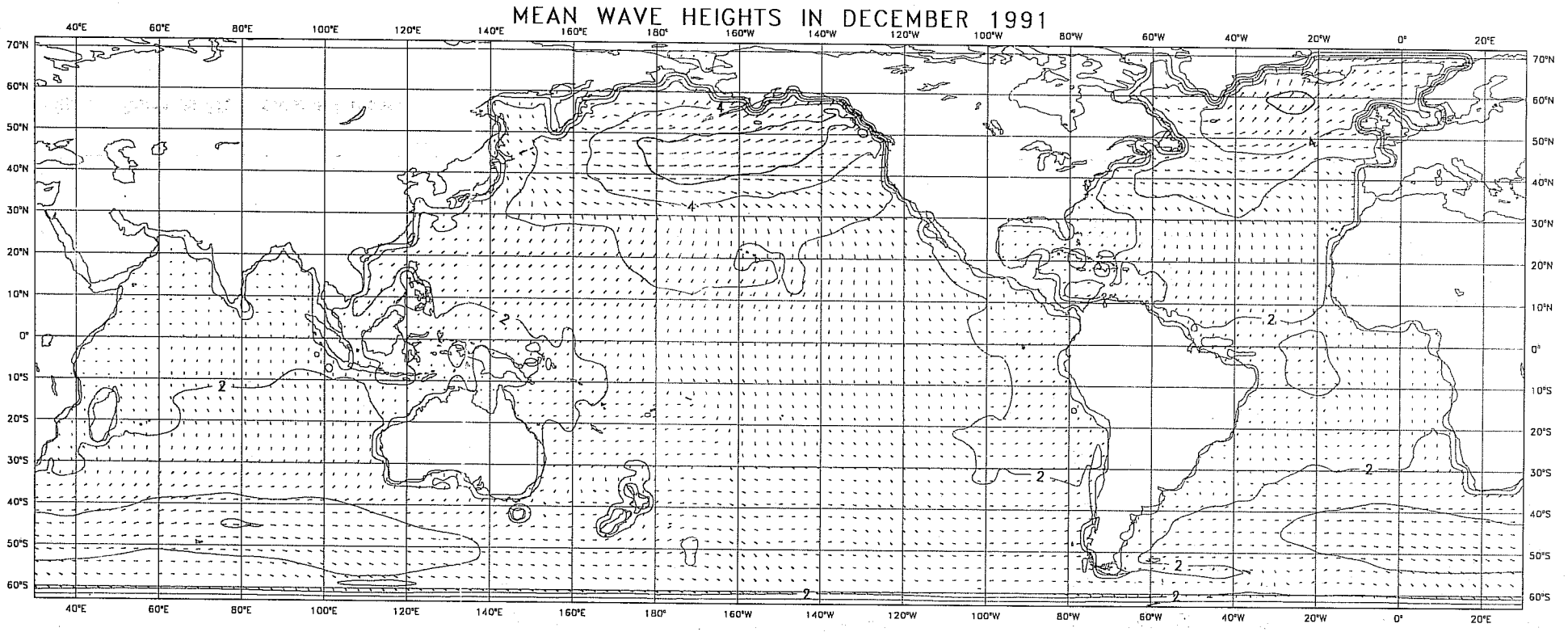

Fig. 3 Global map of mean significant wave height and direction for December 1991 from the WAM model (cycle 4.0) forced by ECMWF's T213 analysed winds.

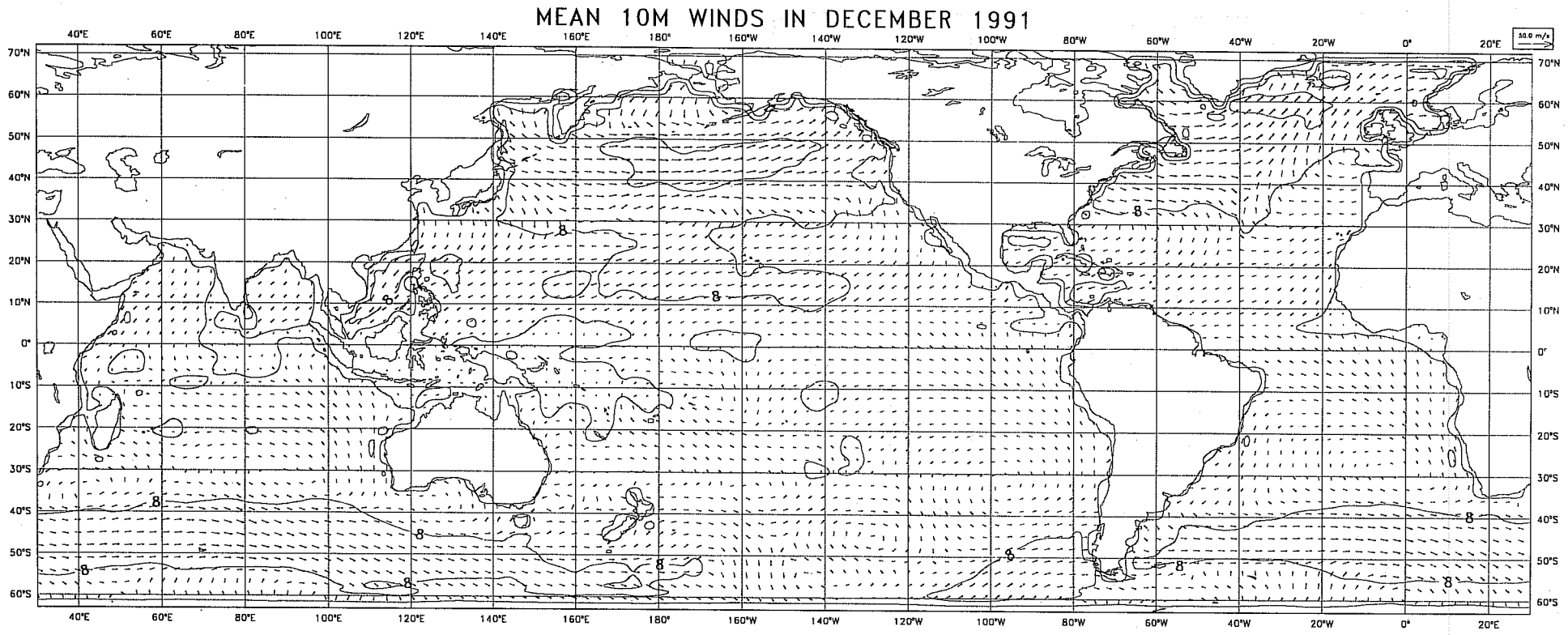

Fig. 4 Global map of mean wind speed and direction for December 1991 from ECMWF's T213 analysed winds, evaluated on the WAM model grid.

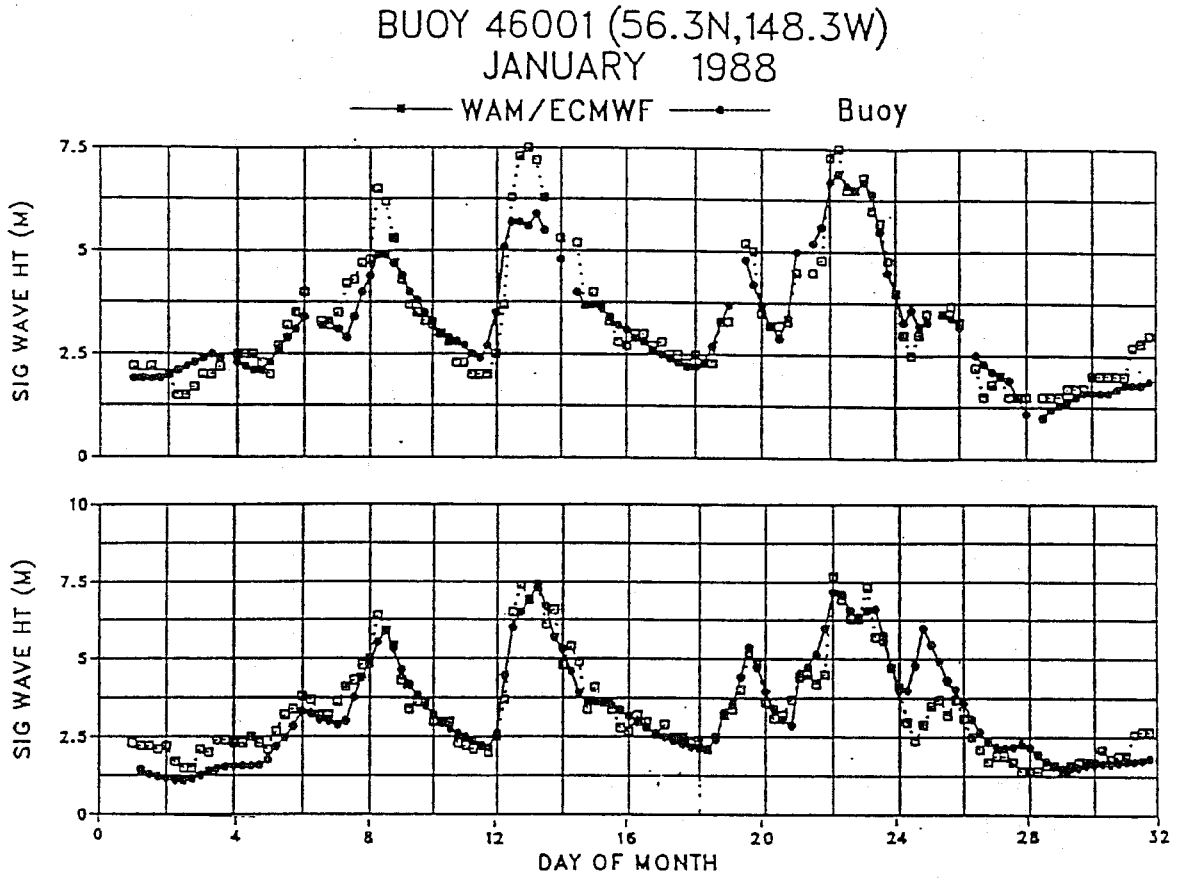

Fig. 5 Time series of WAM model and buoy significant wave heights in November 1988. The upper panel shows interpolated model values, the lower one collocation with the nearest grid point.

collocation method has its shortcomings, and without a close look to the model fields around the buoy location the interpretation of single events may be misleading (see 2.5). Nevertheless the overall model performance can be evaluated in this way.

Since September 1991 buoy wave measurements have been available in real time via the Global telecommunication network and have been used for intercomparison. Table 3 shows the statistics for the last four months of 1991 for 3 areas of the world oceans. Compared to the annual statistics of Zambresky, the number of observations has increased by about 50% and the systematic underprediction of the wave model is considerably smaller. While the standard deviation has increased in the Alaska and Hawaii area and decreased at the US East Coast, the scatter index, which is the standard deviation relative to the data mean, has not changed.

		Alaska	Hawaii	US East Coast
Number		1932 (4657)	1478 (2061)	3150 (4284)
Mean Buoy	(m)	3.34 (3.03)	2.39 (2.14)	1.64 (1.80)
Bias	(m)	-0.13 (-0.22)	-0.05 (-0.28)	-0.08 (-0.38)
STD	(m)	0.71 (0.63)	0.41 (0.37)	0.51 (0.54)
Scatter	(%)	21 (21)	17 (17)	31 (30)

Table 3: Intercomparison statistic with buoy wave height measurements for September 91 to December 91. In brackets are the numbers of Zambresky for December 87 to November 88.

Standard intercomparison plots of measured and computed wave heights, wind speeds and directions at one buoy in each of the areas are given in Figs. 6, 7, and 8. These plots and the statistics included in the figures were produced with the cycle 4.0 version of the wave model and show once more the very good model performance.

Even if this validation is not carried out over a whole year and the actual numbers may change, the progress made with cycle 4.0 driven with ECMWF's T213 analysed wind is obvious. This monitoring of the model performance will continue as part of the operational application in 1992.

2.3.2 Comparison with satellite radar altimeter data

Wave model intercomparisons with buoy measurements are limited, because buoys moorings in the open oceans hardly exist and the number of data is rather small, e.g. Zambresky could only use 13800 data for a one year comparison. Therefore the global performance of the cycle 2.0 wave model was investigated

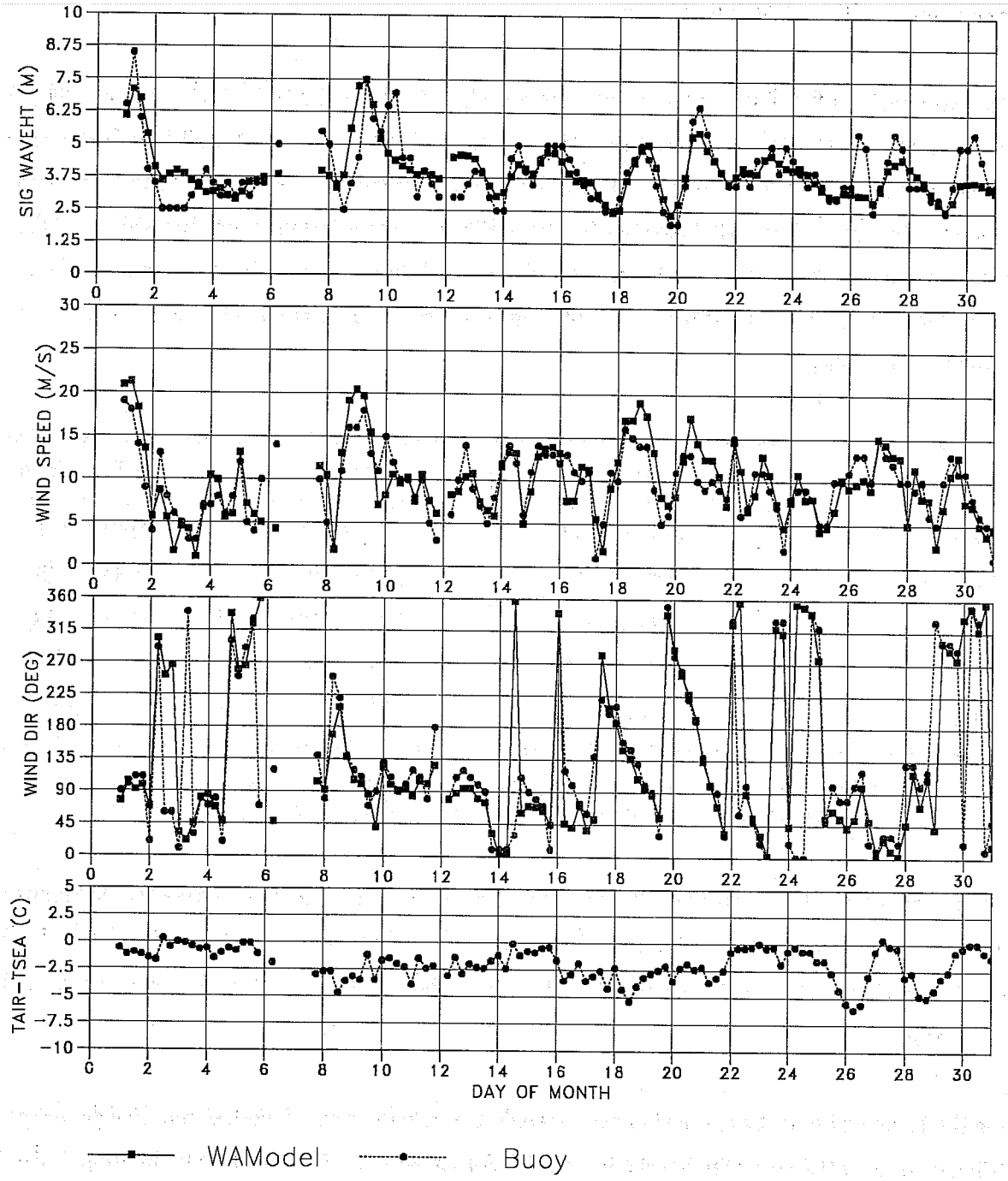

WAVES

MODEL MEAN = 4.0 STDEV = 1.0
BUOY MEAN = 4.0 STDEV = 1.2
LSQ FIT: SLOPE = 0.57 INTR = 1.69
RMSE = 0.84 BIAS = -0.01
CORR COEF = 0.72 SI = 0.21

WINDS

MODEL MEAN = 9.7 STDEV = 4.4
BUOY MEAN = 9.5 STDEV = 3.8
LSQ FIT: SLOPE = 0.90 INTR = 1.19
RMSE = 2.75 BIAS = 0.23
CORR COEF = 0.78 SI = 0.29

Fig. 6 WAM model verification plot and statistics for December 1991 at buoy 46001 in the Gulf of Alaska.

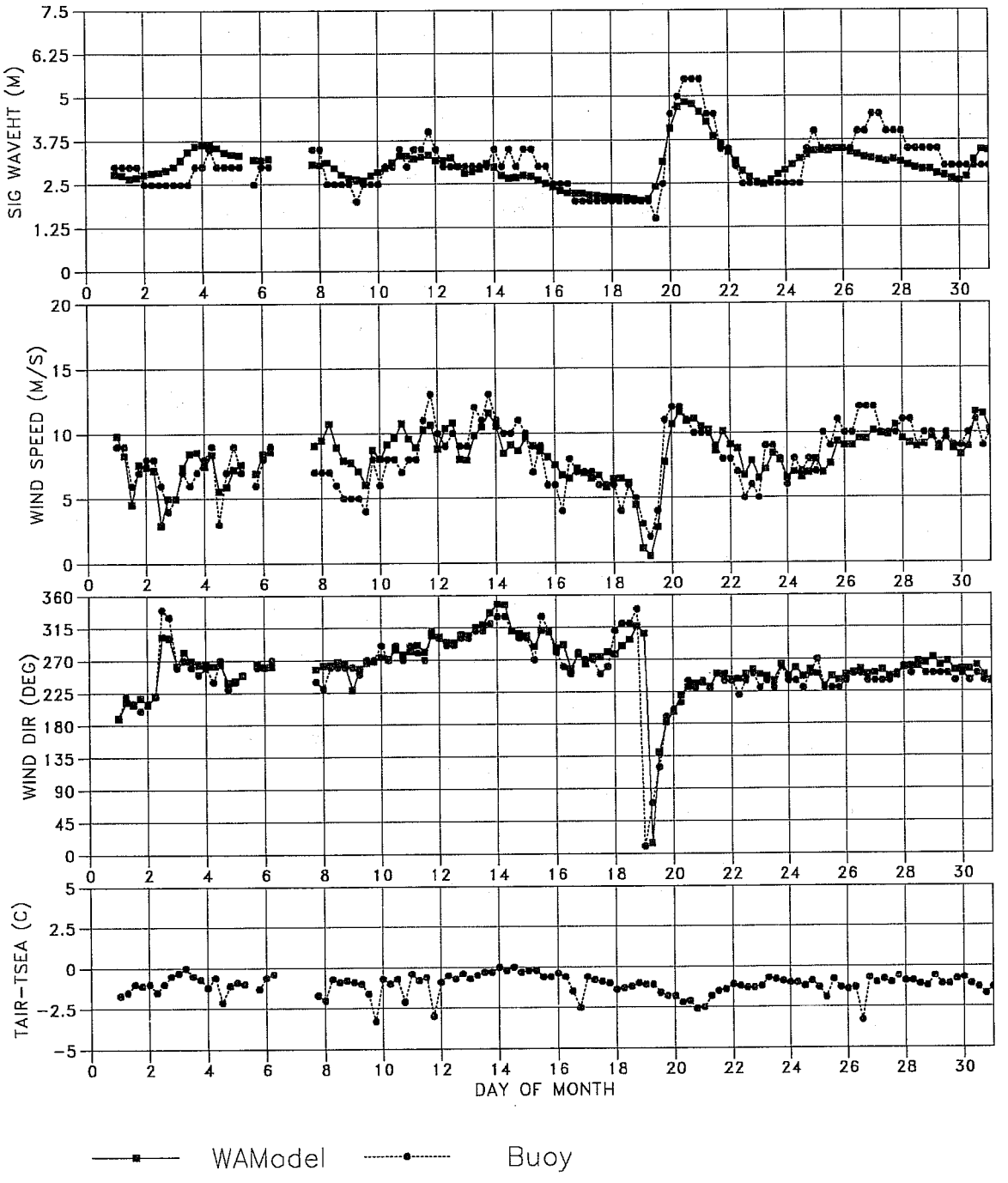

WAVES

MODEL MEAN = 3.0 STDEV = 0.5
BUOY MEAN = 3.1 STDEV = 0.8
LSQ FIT: SLOPE = 0.57 INTR = 1.26
RMSE = 0.46 BIAS = −0.05
CORR COEF = 0.80 SI = 0.15

WINDS

MODEL MEAN = 8.2 STDEV = 2.0
BUOY MEAN = 8.2 STDEV = 2.3
LSQ FIT: SLOPE = 0.65 INTR = 2.92
RMSE = 1.53 BIAS = 0.05
CORR COEF = 0.76 SI = 0.19

Fig. 7 Same as Fig. 6, but buoy 51003 close to Hawaii.

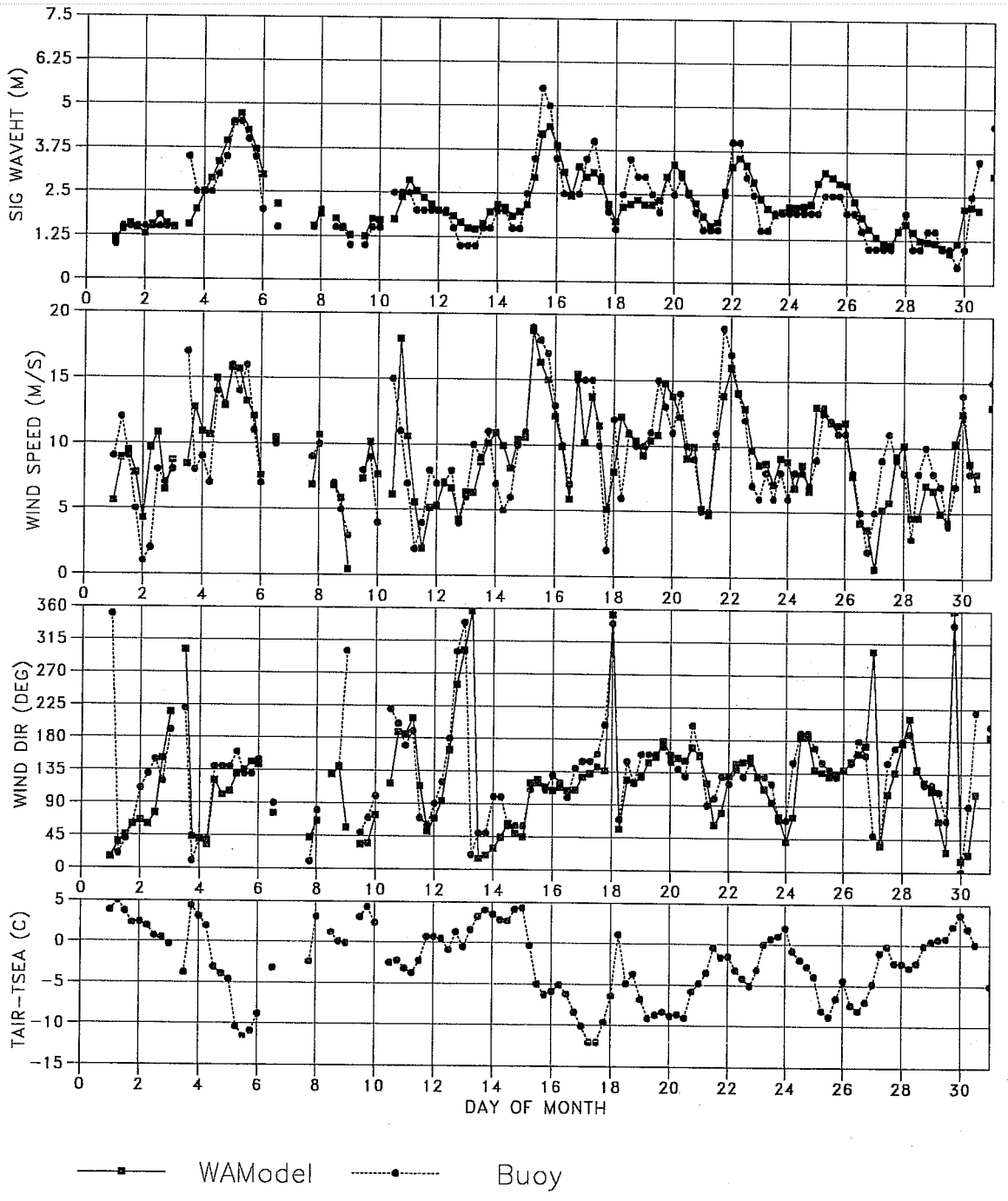

WAVES

MODEL MEAN = 2.3 STDEV = 0.8
BUOY MEAN = 2.2 STDEV = 1.0
LSQ FIT: SLOPE = 0.71 INTR = 0.72
RMSE = 0.53 BIAS = 0.07
CORR COEF = 0.85 SI = 0.24

WINDS

MODEL MEAN = 9.4 STDEV = 3.6
BUOY MEAN = 9.3 STDEV = 3.9
LSQ FIT: SLOPE = 0.68 INTR = 3.00
RMSE = 2.70 BIAS = 0.05
CORR COEF = 0.75 SI = 0.29

Fig. 8 Same as Fig. 6, but buoy 44008 at the US East coast.

by an intercomparison with the radar altimeter of GEOSAT for an entire year (1988), using about half a million collocation data. The complete results are presented by *Romeiser* (1991).

Table 4 shows the significant wave height bias in different areas of the globe averaged over the entire year. The comparison of cycle 2.0 with GEOSAT shows that in the Northern Hemisphere (north of 22 N) the model is 2 cm higher than the altimeter measurements, but 12 cm lower in the Tropics (22 N - 22 S) and 21 cm in the Southern Hemisphere (south of 22 S). This results in a global bias of 13 cm lower than the satellite measurements.

Area	Number	GEOSAT HS (m)	Model HS (m)	Bias (m)
N. Hemisphere	144039	2.09	2.11	.02
Tropics	144747	1.80	1.68	-.12
S. Hemisphere	250328	2.66	2.45	-.21
Global	539114	2.28	2.15	-.13

Table 4: Significant wave height bias in 1988 from the GEOSAT altimeter comparison.

The analysis of this model behaviour leads to the following conclusions:

- The underprediction in the southern hemisphere may be related to an underestimation of the driving wind fields in this data spare area, and to the model land boundary at 63 S, which does not allow sufficient growth especially when the ice border is located far more to the South.

- In the Northern Hemisphere where the best wind field quality is expected, the overall bias is negligible. This is in contrast to buoy intercomparisons (see Table 3) which indicate an under-prediction by the wave model. A possible explanation is that the altimeter measurements are too low in high seastates (*Dobson et al.*, 1987 and *Guillaume and Mognard*, 1991).

- The underprediction in the tropics is mainly caused by an underprediction of swell arriving from the extratropical areas. This is partly related to the problems outlined above for the southern hemisphere and partly to the propagation scheme and dissipation source function used in cycle 2.0 of the wave model. It basically confirms the results found at the buoys around the Hawaii Islands (see Table 3)

- An intercomparison of cycle 4.0 with the first calibrated ERS-1 altimeter data was done for December 1991. Table 5 and Fig. 9 indicate the same trend in the bias as the GEOSAT intercomparison, but cycle 4.0 has higher wave heights relative to ERS-1 than cycle 2.0 relative to GEOSAT.

Area	Number	ERS-1 HS (m)	Model HS (m)	Bias (m)
N. Hemisphere	5613	3.16	3.45	.28
Tropics	7812	2.07	2.12	.05
S. Hemisphere	11264	2.57	2.50	-.07
Global	24689	2.55	2.60	-.05

Table 5: Significant wave height bias in December 1991 from the ERS-1 altimeter comparison.

This result indicates that the modifications done to the wave model and the driving wind fields are in the right direction. A direct comparison of cycles 2.0 and 4.0 driven with the same winds results in a similar increase of the global mean wave heights. If the model buoy intercomparisons are taken into account, it can be concluded, that the altimeters of the two different satellites have a very similar performance in underestimating the higher seastates.

2.4 Intercomparison with the UK Met. Office model

The separation of wave model errors and errors in the driving wind fields is one of the most important points in verification studies. Because most of the measured wind speeds are assimilated in the wind fields no independent data is available for verification. In addition the wave field at a particular site depends on the space and time structure of the winds, e.g. errors in storm location and strength influence the prediction of swell several days later and far away from the original generation area.

One way to address this problem is to carry out a four-way model intercomparison. *Günther and Holt* (1992) report on intercomparison of the third generation WAM model (cycle 3.0) and the second generation wave model of the UK Met. Office. Both models were forced by the ECMWF winds and by the UKMO winds for November 1988. The models were run on the same 3 degree latitude-longitude grid with an angular resolution of 15 degrees.

Because the 'official' reference height for the wind fields is different (10 m at ECMWF and 19.5 m at UKMO) the winds were rescaled by 9%. Comparison with the buoy measurements indicates that both wind

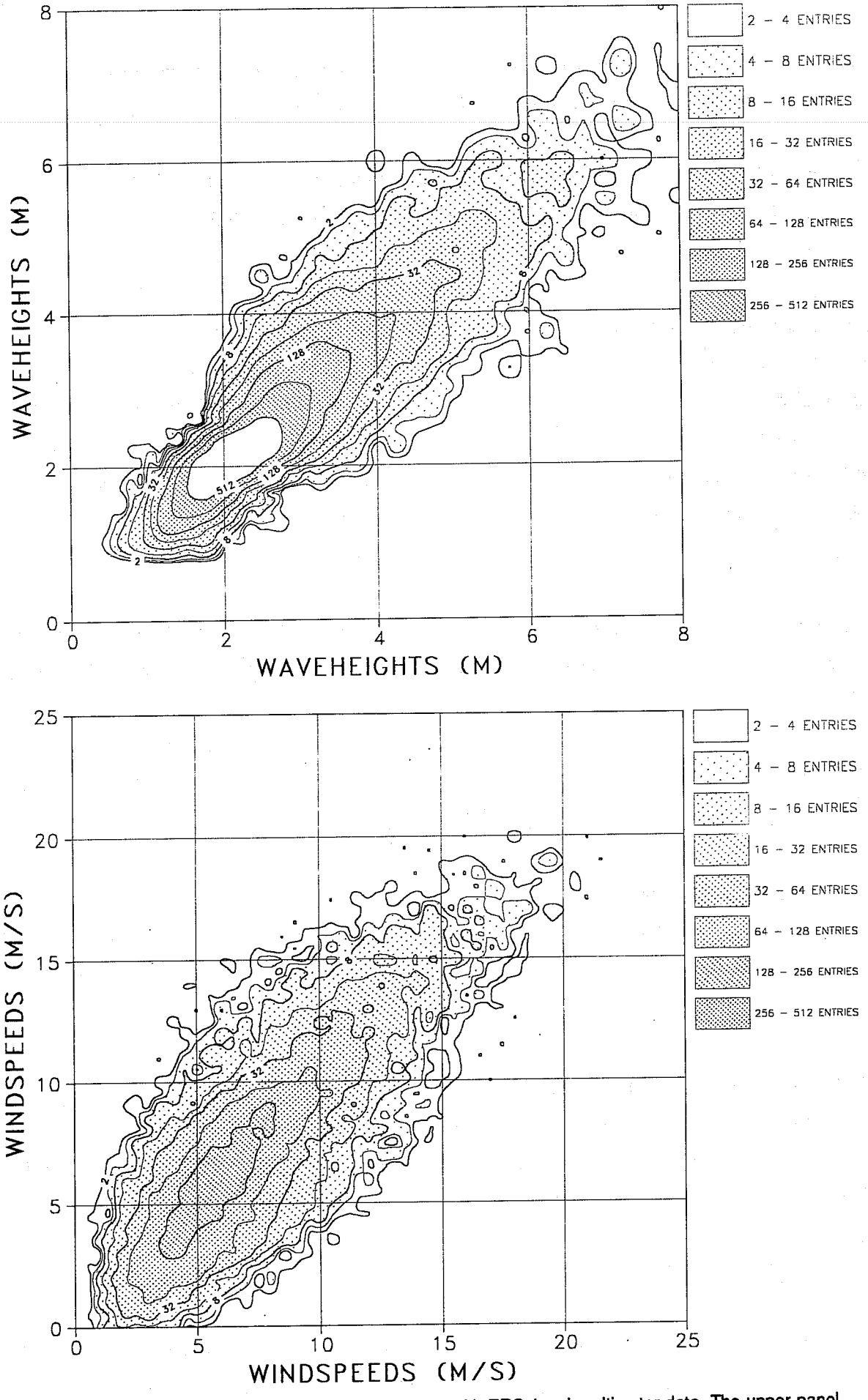

Fig. 9 Intercomparison of the WAM model (cycle 4.0) with ERS-1 radar altimeter data. The upper panel shows wave height, the lower one wind speeds.

fields show the same biases, which implies that both wind assimilation systems treat buoy data very similarly and do not adjust the observations to the 'official' reference height.

The comparison with buoy measurements showed that both models driven with their own winds performed well in the North-West Atlantic, an area of primarily fetch and duration limited growth. The 2-D model spectra are in good agreement, and very similar directional relaxation in turning winds was found.

In the Central and North-East Pacific, areas where swell was important, both models were systematically low. The wave heights of the WAM model were lower than the UKMO model. In contrast the mean periods of the WAM model were much closer to the measurements than the UKMO model periods, which were systematically short. The 2-D spectra in both models show similar structures. Frequency and angular distributions are similar, but indicating a stronger turning for swell propagating over long distances and more peaked angular swell distribution in the UKMO model. Because measurements of 2-D spectra do not exist, the cause of the systematic under-prediction could not be identified.

Comparison of the 1-D buoy spectra with the model spectra showed that the UKMO model is particularly deficient in swell energy at the middle frequencies around 0.1 Hz, probably originating from the swell separation method (*SWAMP*, 1985). In the presence of swell the development of wind waves in the WAM model is slow compared to the UKMO model and observations. The strong non-linear interactions between wind waves and swell propagating in the same direction may affect the energy balance at high frequencies and prevent the development of a second peak.

2.5 High resolution experiments

In chapters 2.1 and 2.2 general statistics of wave model comparisons with buoys and satellite have been presented. No effort was made to discuss the model performance in special cases like major storms or swell events.

The standard model is running with a 3 degree resolution in latitude and longitude, a 30 degree angular resolution of the wave spectrum and with 25 logarithmically spaced frequencies covering 0.0418 Hz to 0.411 Hz. Especially the coarse spatial and angular resolution was often criticised and in very extreme events an extension towards lower frequencies was discussed.

A series of model experiments were done to investigate this.

- the entire November 1988 was rerun with an angular resolution of 15 degrees. The effect was an increase of 0.11 m of the mean global wave height. This increase occurred not only in swell areas,

as expected because of the improved propagation characteristics. The wind waves where affected in the same way. Changes up to 0.5 m could be observed at individual grid points and times, which reduces the bias in the buoy comparison statistics (see Table 6).

		Alaska	Hawaii	US East Coast
Number		356	356	367
Mean Buoy	(m)	4.10	2.57	2.18
Bias	(m)	-0.36 (-0.49)	-0.32 (-0.40)	-0.30 (-0.35)
STD	(m)	0.79 (0.87)	0.47 (0.45)	0.45 (0.44)
Scatter	(%)	19 (21)	18 (18)	21 (20)

Table 6: Intercomparison statistic with buoy wave height measurements for November 88, obtained by a 15 degree angular resolution cycle 3.0 model run. In brackets are the numbers for the standard 30 degree model.

- The second experiment was a rerun of November 1988 with a latitude, longitude resolution of 2 degrees. The angular resolution remained 30 degrees. As above the buoy intercomparison was only changed marginally. But the peak wave heights in extreme storms increased by up to 1 m, due to the better resolved peaks in the forcing input wind fields. The analysis of a major storm north-west of the Hawaii islands clearly shows this benefit. In addition it demonstrates how important the intercomparison of the wave pattern around the buoy location is for the analysis of model behaviour. Fig. 10 shows the model results at the four surrounding grid points of buoy 51001. Whereas panel A is the closest gridpoint to the actual measuring position, the best intercomparison is achieved in panel C, indicating a misplacement of the storm by about one grid point or 150 km to the North-West.

- In a third experiment four low frequencies were added, extending the frequency range to .0285 Hz (*De las Heras*, 1990, *De las Heras and Janssen*, 1991). The model was applied to an extreme storm in the north west Pacific generating very long period swell. Measurements in the Gulf of Alaska, Hawaii and at the coast of Peru showed periods well above 20 S, corresponding to frequencies less than .05 Hz. The standard model and the model with the extended frequency range were not able to generate the low frequency swell, a tendency which was already noticed in other intercomparisons. A rerun with new source functions of cycle 4.0 could improve the results, but the coarse (3 degree) latitude longitude and 30 degree angular resolution probably prevent a total success.

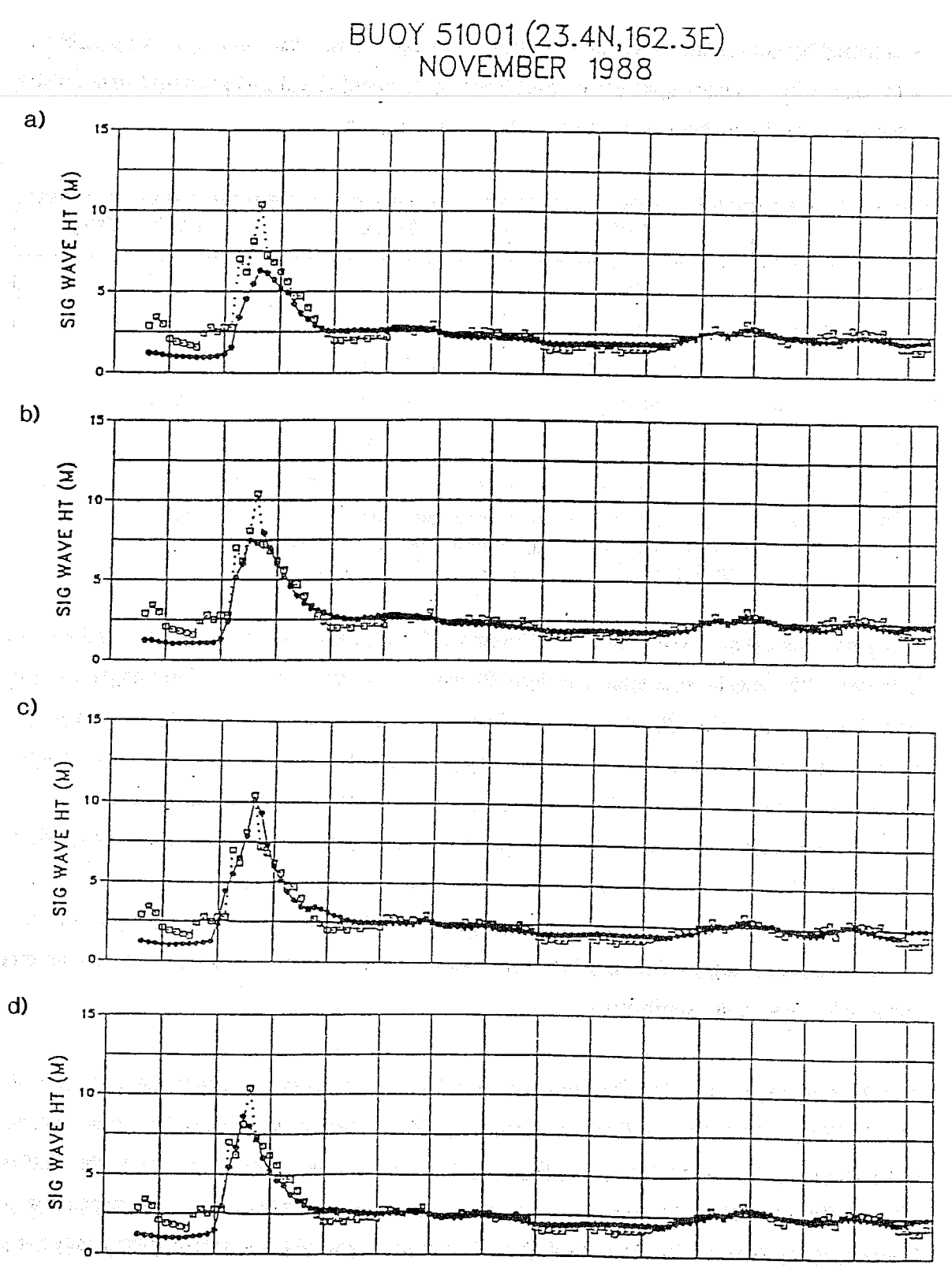

Fig. 10 Wave height intercomparison in November 1988 between buoy 51001 measurements and WAM model (cycle 4.0) results at the surrounding grid points. (a) 23°N, 162°W; (b) 23°N, 164°W; (c) 25°N, 164°W; (d) 25°N, 162°W.

2.6 A five day forecast experiment

So far all model intercomparison studies used ECMWF's analysed wind fields to drive the model. The wave analysis fields generated in this way are the initial fields from which the model starts to compute the wave forecasts, using the forecast wind from the atmospheric model. Therefore the accuracy of the initial fields (investigated above) and the quality of the forecast winds determine the forecast performance. Especially the long memory of the swell requires very good initial fields, which can be improved by wave data assimilation systems, as discussed in the next chapter.

In this chapter the wave model forecast fields are compared to the corresponding analysis fields, to investigate the errors introduced by the wind forecast error. The cycle 3.0 of the wave model was applied to simulate an operational 5 day forecast for November 1988.

Table 7 summarizes the regional and global statistics of wave heights and wind speed differences between forecasts and analysis, averaged over 25 days. Whereas the forecast wind speeds are normally higher than the analysed (positive bias), most of the wave height biases are negative, indicating a slightly too strong dissipation or too small growth in the wave model. This is supported by the extent of the 2 m wave height line in Figs. 11 and 12 which show the mean analysed and mean 5 day forecast wave heights, respectively.

	N. Hemisphere		Tropics		S. Hemisphere		Global	
day	Hs(m)	U(m/s)	Hs(m)	U(m/s)	Hs(m)	U(m/s)	Hs(m)	U(m/s)
1	.00	.25	-.01	.10	-.04	-.01	-.02	.09
2	.02	.40	-.01	.19	-.04	.07	-.01	.19
3	.01	.43	-.01	.26	-.04	.06	-.02	.22
4	-.01	.41	-.02	.20	-.05	-.01	-.03	.16
5	-.03	.42	-.03	.12	-.08	-.12	-.06	.09

Table 7: Mean forecast - analysis wave heights and windspeed in November 88 for different regions and forecast periods.

The wave height biases (less than 10 cm) are quite small compared to the results obtained with the GEOSAT intercomparison (Table 4). The other global statistics for the 5 day forecast are a root-mean-square error of 64 cm, a scatter index of 25% and correlation coefficient of .57 (*Carretero and Günther*, 1992). This indicates that even after 5 days the forecast is close to the analysis.

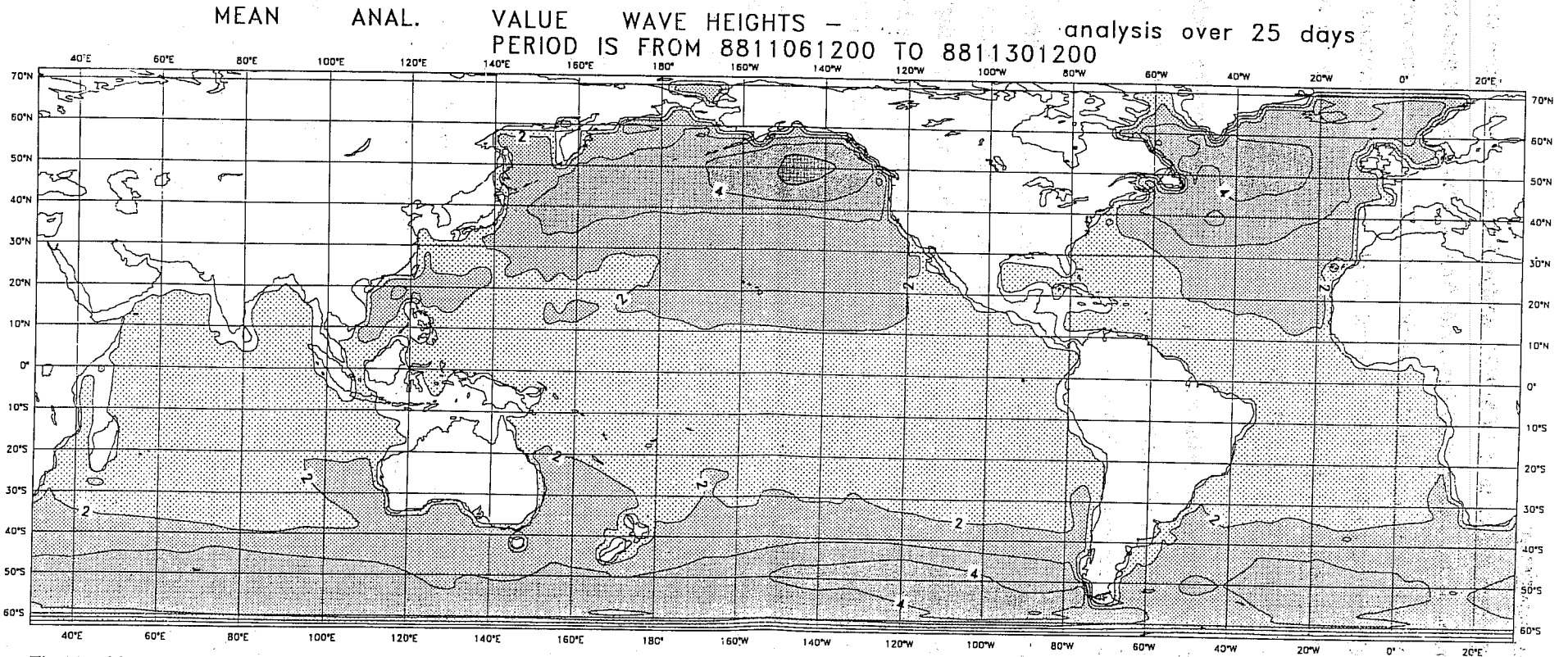

Fig.11 Mean analysed wave height in November 1988.

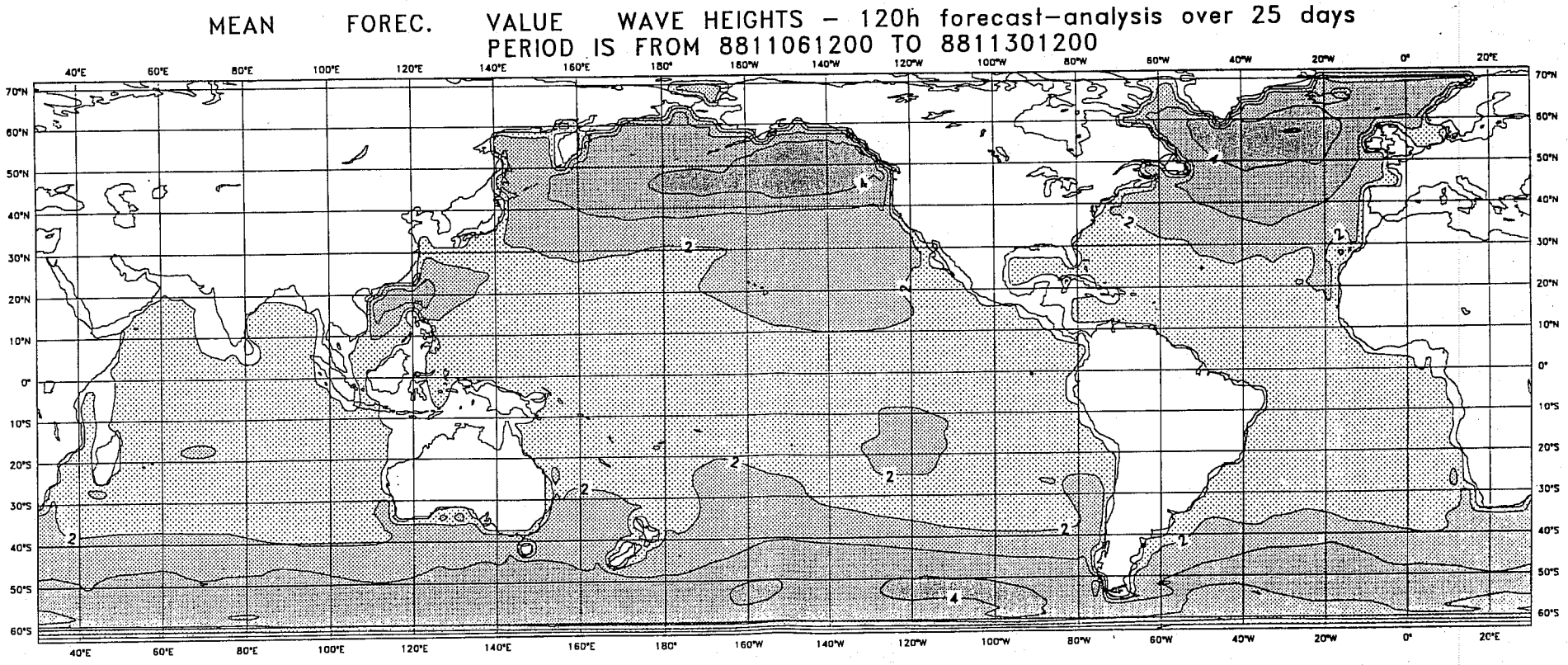

Fig.12 Mean 5 day forecast wave height in November 1988.

3. DATA ASSIMILATION

Wave model initial fields are normally generated by forcing the model with analysed wind fields which benefit from the data assimilation in the atmospheric models. This is possible, because wave models are losing the information provided by the initial fields in a couple of days. Therefore assuming that the wind fields and wave model are correct, a wave data assimilation is not required. In addition the impact of the few available buoy measurements into the initial fields was considered as very small.

The launch of oceanographic satellites which provide extensive data sets covering the whole model area has changed the situation completely. A considerable improvement of the model performance is now expected from wave data assimilation.

In the following a brief description of the assimilation system is outlined and the results of a number of applications are summarized. A full documentation of the work is included in *Lionello et al.* (1992a).

3.1 Method

In continuation of the work of *Janssen et al.* (1989) the wave data assimilation system is based on Optimal Interpolation to blend the measured wave heights and wind speeds into the model fields. Optimal interpolation is a standard method and its application is straight forward, but it is necessary to define the correlation length (radius of influence) and the relative weight of model and measurement. An extensive study has been done to determine the optimal values.

The wave model however uses spectra with around 300 components as prognostic variables. The main problem is to change these in a consistent way. This means additional assumptions have to be used in agreement with internal model relations, e.g. a simple rescaling of the spectral components without changing the energy distribution over frequencies results in a very rapid loss of the information provided by the measurements. In addition to that it is essential to update the driving winds consistent to the wave model growth curve as well, which opens the possibility to feed back updated winds to the atmospheric model.

A full description of the method and applications to SEASAT and GEOSAT altimeter data are in *Lionello et al.* (1992a, 1992b).

A statistical evaluation of the GEOSAT assimilation for November 88 (*Carretero and Günther*, 1992) demonstrates the impact to the model analysis fields, Fig. 13 shows differences of mean wave heights in November 88. Most obvious is the increase of heights in the Indian ocean (.5 m) and in the South East Pacific (.4 m), and a decrease of .4 m in the North East Pacific. These changes are in agreement with the analysis of *Romeiser* (1991) (see 2.3.2), and lead of course to the same conclusions.

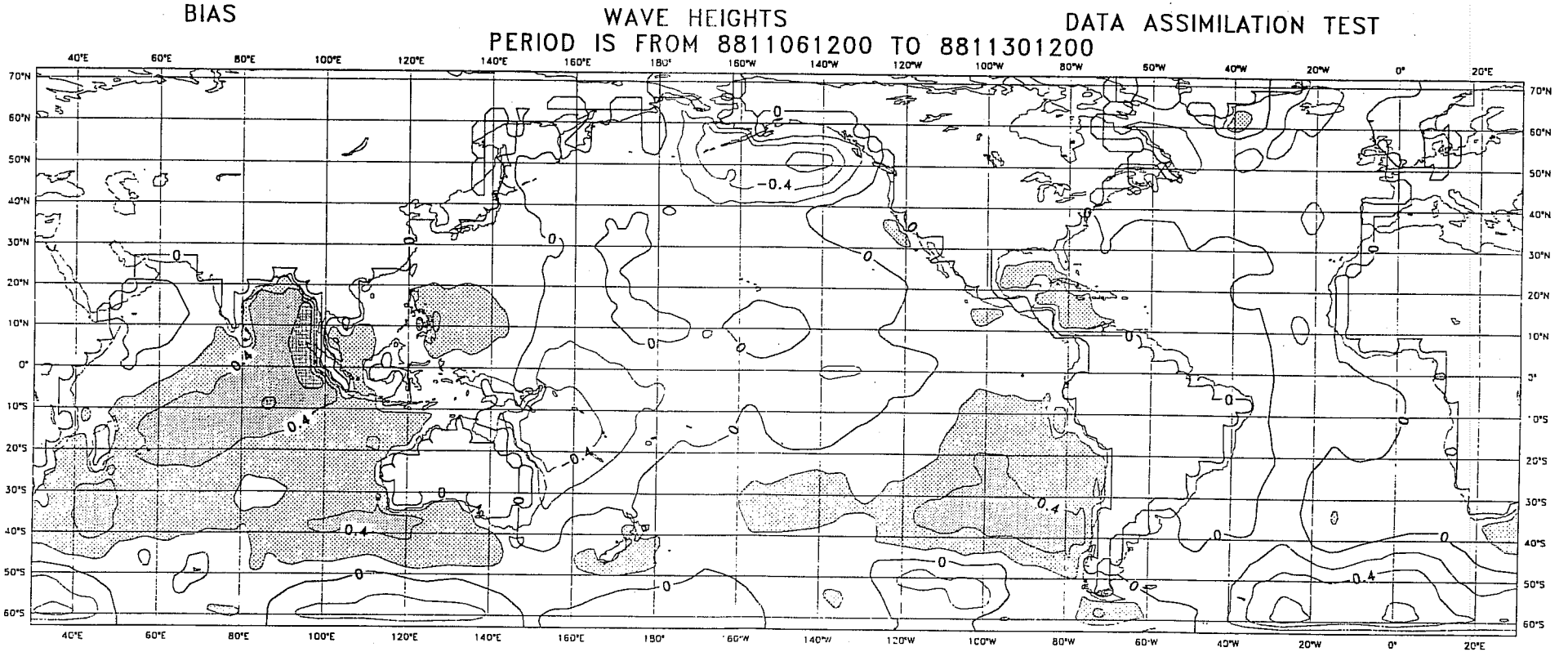

Fig.13 GEOSAT assimilated wave heights minus analysis in November 88.

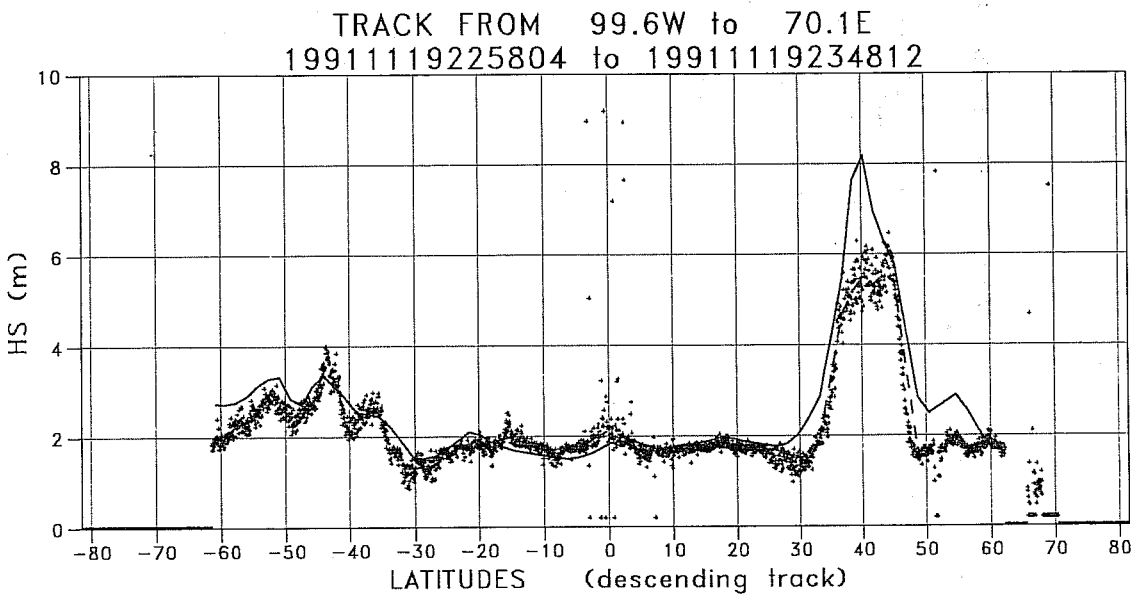

Fig.14 ERS-1 radar altimeter quality control plot. Track from (80 S, 99.6 W) to (80 N, 70.1 E) on 19. Nov. 1991.

3.2 Data organisation and quality control

An essential part of an operational wave data assimilation system is the data organisation and quality control. In collaboration with the UK Met. Office FM94 BUFR codes for all data products of the ERS-1 satellite have been developed. The data formats are used by ESA to distribute the fast delivery data of ERS-1 to member states and ECMWF's operational data acquisition and file management system provided easy access to the measurements.

The data quality control for radar altimeter has been developed based on earlier work with SEASAT data (*Bauer et al.*, 1992). The purpose is to identify unrealistic data by statistical methods , mainly spikes in the vicinity of islands and sea ice fields. Fig. 14 gives an example from an ERS-1 track over the Pacific. The unrealistic measurements around 70 S are taken over ice. The spikes at the equator are caused by islands (not resolved in the wave model grid). The dark part north of 65 N is related to Alaska and ice. The two curves are model and altimeter wave heights. Both are in good agreement over most of the Pacific, only the storm at 40 N is over estimated by the model (or more likely under-estimated by the altimeter).

3.3 Application to ERS-1 radar altimeter data

The assimilation system was applied in quasi real time to support the ERS-1 calibration and validation. The altimeter data were passed through the assimilation in a passive way, so they could not effect the analysis. The data quality control (Fig. 14) and the intercomparison with the wave model (Fig. 9) has been very effective to identify errors and problems in the ESA altimeter software and model function.

First tests of the complete assimilation system with uncalibrated data have been technically successful. Further test with reliable ERS-1 altimeter data have to be done to investigate the impact on the forecast of the global wave field.

4. INTERACTION OF WINDS AND WAVES

This work was started when it was realised that surface gravity waves and its associated momentum flux might be important in controlling the shape of the wind profile over ocean waves.

As a matter of fact the common belief in the field was that air turbulence was dominating the wind profile and the effect of surface gravity waves was regarded to be small. However, *Snyder et al.* (1981) found that the momentum transfer from wind to waves might be considerable so that the associated wave-induced stress may be a substantial amount of the total stress in the surface layer. This suggested that the velocity profile over sea waves may deviate from the usual profile of turbulent air flow over a flat plate. As a consequence the drag coefficient at 10 m height should depend on the sea state. Typically, young wind sea corresponds to a sea state with steep waves as many breaking events occur while old wind sea is rather smooth. This results in variations of the drag coefficient of about a factor of two (cf. e.g. *Donelan*, 1982; *Maat et al.*, 1991). *Janssen* (1989) finally determined the wave age dependence of the drag coefficient by means of the quasi-linear equations of wind wave generation in which the shape of the wind profile was determined by both turbulent fluxes and the wave-induced stress. Again, a sensitive dependence of the drag coefficient on the sea state was found.

Waves, storm surges and the weather depend sensitively on knowledge of the surface stress. As waves play an important role in the magnitude of the surface stress, it seems natural to determine the stress in a self-consistent manner by allowing the drag coefficient to be dependent on both wind speed and the sea state. Consequences of this approach for surface gravity waves have been discussed in some detail by *Janssen* (1991). Some of its results will be briefly discussed below.

In addition, taking analysed wind fields which are supposed to be of high quality, *Mastenbroek et al.* (1991) coupled a storm surge model with the WAM model cycle 4.0 and found favourable agreement during peak event surges, which could be ascribed to a more realistic determination of the surface stress. Also *Weber et al.* (1991) coupled the WAM model with the MPIfM version of the European centre weather model. For a perpetual July run some impact of the ocean waves on the general circulation pattern could be detected.

All this suggests that it is important to have a realistic description of the momentum transfer at the air-sea interface. It is therefore relevant to investigate possible impact on wave prediction.

The parametrization of the quasi-linear results of the input source function and the sea state dependence of the drag coefficient through the so-called wave-induced stress have been given in *Janssen* (1991). Briefly, the wind input term is given by

$$S_{in} = \gamma F$$

where F is the two-dimensional frequency spectrum and γ the growth rate of the waves. From *Miles* (1957) we know that for a logarithmic wind profile γ depends on only two parameters, namely

$$x = u_* \cos(\theta-\phi)/c \text{ and } \Omega = gz_o/u_*^2$$

with u_* the friction velocity, θ the direction in which the waves propagate, ϕ the wind direction, c the phase speed of the waves and z_o the roughness length. Thus, through Ω the growth rate depends on the roughness, which in its turn depends on the sea state. The growth rate, normalised by the angular frequency ω, is given as

$$\frac{\gamma}{\omega} = \varepsilon\beta x^2$$

where

$$\beta = \frac{\beta m}{\kappa^2}\mu \ln^4(\mu),\ u < 1$$

with κ the von Karman constant, $\beta m = 1.2$ a constant and μ the dimensionless critical height $\mu = kz_c$ (with k the wave number and z_o the critical height defined by $U_o(z=z_c) = c$).

The stress τ of air flow over sea waves depends on the sea state and from a consideration of the momentum balance of air it is found that τ is given as

$$\tau = C_D U^2(L)$$

with drag coefficient

$$C_D = \{\kappa/\ln(L/z_o)\}^2$$

where

$$z_o = \frac{\alpha\tau}{g}/\sqrt{(1-\tau_w/\tau)}.$$

Here, L is the mean height above the waves and τ_w the wave-induced stress given by

$$\tau_w = \rho_w \int df d\theta\ \omega\ \gamma\ F \cos(\theta-\phi).$$

In practice, as the major contribution of wave stress is carried by the high-frequency waves which respond quickly to changes in wind speed and direction, the wave stress is pointed in the wind direction. The constant α is chosen in such a way that for old wind sea the usual Charnock relation for the drag over sea waves is found. This avoids double counting problems.

As the wave stress depends in a sensitive manner on the high-frequency part of the spectrum, much attention was devoted to a proper description of the high-frequency tail of the spectrum. It was found that, especially for old wind sea, the WAM model cycle 2.0 gave too high high-frequency levels. This was ascribed to an improper energy balance in this range which could be corrected by modifying the wave breaking dissipation. Thus

$$S_{dis} = -\gamma_d F$$

where

$$\gamma_d = \tfrac{1}{2} c_{dis} \langle\omega\rangle (\langle k\rangle^2 E)^2 \left(\frac{k}{\langle k\rangle} + \left(\frac{k}{\langle k\rangle} \right)^2 \right).$$

Here $c_{dis} = 4.5$ is a constant, E is the total wave variance and $\langle\omega\rangle$ and $\langle k\rangle$ are mean angular frequency and mean wave number.

Next, the new version that emerged which was called ATMWAM was subjected to a number of tests, namely SWAMP2, simulating the JONSWAP experiment and the November 1988 hindcast. The ATMWAM model gave generally a more realistic fetch dependence especially regarding the Phillips constant, which is a measure of the high-frequency content. The November 1988 hindcast showed a somewhat better performance of the ATMWAM model regarding verification statistics of wave height.Both bias and rms error were somewhat smaller for ATMWAM than for the WAM model.

It was concluded that the ATMWAM model (now called WAM cycle 4.0) was found to be a reliable tool ready for doing two interaction experiments with the atmospheric model. It is expected to give a realistic description of momentum transfer at the air-sea interface, which is corroborated by a recent comparison of observed and theoretical stresses (*Janssen*, 1991). In addition, some improvements in wave height prediction have been found.

5. SUMMARY AND CONCLUSIONS

The third generation WAM wave model was extensively tested and technically and physically improved. The final cycle 4.0 version has become the standard model of the WAM group. It has been implemented in ECMWF operational forecasting system together with the required archiving and diagnostics software. The distribution of 10 day wave forecast products will start in 1992 as part of ECMWF's optional wave program.

The cycle 4.0 of the WAM model is organised as a subroutine version. It needs less computer resources than cycle 2.0. Total memory use and input/output could be reduced by about 30% and 75%, respectively. The CPU time only decreased by 10% because of the new propagation scheme and source functions.

The cycle 4.0 was extended by a number of new options. The program allows computations on a nested grid. Depth and current refraction can be activated.

New input and dissipation source functions have been developed and introduced into cycle 4.0. These take into account that the wind profile and therefore momentum flux through the sea surface is seastate dependent. Tests with atmospheric and surge models coupled with the WAM model have demonstrated the benefits.

The model was extensively verified against buoy and satellite altimeter measurements. The cycle 4.0 of the wave model forced by the T213 windfields of ECMWF agrees remarkably well with buoy and satellite wave height data. In particular:

- Comparison of cycle 4.0 with buoys show less bias (about 10 cm) than cycle 2.0 (about 25 cm) and the scatter index has slightly decreased to about 20%.

- The systematic underprediction of wave heights in the tropics and at the buoys around Hawaii was not observed anymore.

- The underprediction of extreme wave heights with cycle 2.0 could be traced. Two main reasons were found: the grid resolution of 3 degrees, and misplacement of storms in the wind fields. Collocating buoys with the nearest grid point instead of interpolating to the buoy position avoids artificial shadowing for buoys close to the coast.

- A 15 degree angular resolution run produced better agreement with buoy measurements at least with the cycle 3.0 version.

- 1-D wave spectra comparisons indicate a reduced growth of wind wave development in the presents of swell in the same direction. This was found with the cycle 3.0. The cycle 4.0 performance has to be investigated.

- Evidence was found that the altimeters of GEOSAT and ERS-1 underestimates high seastates.

- From the satellite intercomparisons in the Southern Hemisphere it is concluded that the model grid has to be extended to the ice-edge.

- ECMWF's wind speeds are in very good agreement with the ERS-1 altimeter measurements and with buoy observations. A systematic error was not found.

A wave and wind data assimilation system based on Optimal Interpolation was further developed and combined with the wave model. The use of different methods to update swell and windsea and the accurate fit to model growth curves resulted in a longer persistence and better intercomparisons. At present the wave heights and wind speeds are assimilated only. An extension for wave periods and directions should be carried out, when these data become available on a global scale, e.g. from the ERS-1 wave scatterometer.

The combined wave prediction and assimilation system is ready for operational use. It was successfully applied in a quasi operational mode during the calibration/validation phase of ERS-1 to monitor the performance of the satellite's altimeter. Especially the quality control package has proven to be very successful to trace errors. Due to the delayed launch of the satellite impact studies with calibrated ERS-1 data had to be shifted into 1992.

A five day forecast experiment has demonstrated the high accuracy of the WAM model forced by ECMWF's wind fields. Therefore it can be expected that the operational application of the model in 1992 will be a success.

Acknowledgements

The work described in this report has been carried out under European Communities Contract No. SC1-0013-C(GDF)(SC1000013).

References

Bauer, E., S. Hasselmann, K. Hasselmann, H.C. Graber (1992): Validation and assimilation of Seasat altimeter wave heights using the WAM wave model. J.G.R. in press.

Carretero, J.C. and H. Günther (1992): Wave forecast performed with the WAM model at ECMWF. Statistical analysis of a one month period (November 1988). Internal report of Programa de Clima Maritimo, Direccion General de Puertos y Costas. MOPU. In preparation.

De las Heras, M. (1990): WAM hindcast of long period swell. KNMI Memorandum 00-90-07.

De las Heras, M. and P.A.E.M. Janssen (1991): Comparison of hindcast results of low-frequency swell with the WAM and coupled WAM model. KNMI Memorandum 00-91-07.

Dobson, E., F. Monaldo, J. Goldhirsh and J. Wilkerson (1987): Validation of Geosat altimeter-derived wind speeds and significant wave heights using buoy data. Johns Hopkins APL Technical Digest, Vol. 8, No. 2, 222-233.

Donelan, M.A. (1982): The dependence of the aerodynamic drag coefficient on wave parameters. Proc.First International Conference on Meteorology and Air-Sea Interaction of the Coastal Zone, The Hague. Boston, Amer.Meteor.Soc., 381-387.

Guillaume, A. and N.M. Mognard (1991): A new method for the Validation of Altimeter-derived Sea State Parameters with results from Wind and Wave Models. Accepted for publication in J.Geoph.Res.

Günther, H., S. Hasselmann and P.A.E.M. Janssen (1992): The WAM model Cycle 4.0. User Manual. Deutsches Klima Rechen Zentrum, Technical Report No. 4.

Günther H. and M. Holt (1992): Intercomparison of the WAM and UKMO wind wave model. In preparation.

Janssen, P.A.E.M. (1989): Wave-induced stress and the drag of airflow oversea waves. J.Phys.Ocean., 19, 745-754.

Janssen, P.A.E.M., P. Lionello, M. Reistad, A. Hollingsworth (1989): Hindcast and data assimilation studies with the WAM model during the Seasat period. J.Geoph.Res., 94, 973-993.

Janssen, P.A.E.M. (1991): Quasi-linear theory of wind-wave generation applied to wave forecasting. J.Phys.Ocean., 21, 1631-1642.

Janssen P.A.E.M. (1991): Experimental evidence of the effect of surface waves on the air flow. Submitted for publication.

Lionello, P., H. Günther and P.A.E.M. Janssen (1992a): Assimilation of altimeter data in a global third generation wave model. ECMWF Technical Report No.67. Reading, ECMWF, 88 pp.

Lionello, P., H. Günther and P.A.E.M. Janssen (1992b): Assimilation of altimeter data in a global third generation wave model. Accepted for publication in J.Geoph.Res.

Maat, N., C. Kraan and W.A. Oost (1991): The roughness of windwaves. Bound.Layer.Meteor., 54, 89-103.

Mastenbroek,C., G. Burgers and P.A.E.M. Janssen (1991): The dynamical coupling of a wave model and a storm surge model through the atmospheric boundary layer, submitted.

Romeiser R. (1991): Validation of the WAM wave prediction model by Geosat wave height data. Submitted to J.Geoph.Res.

Snyder, R.L., F.W. Dobson, J.A. Elliott and R.B. Long (1981): Array measurements of atmospheric pressure fluctuations above surface gravity waves. J.Fluid Mech., 102, 1-69.

SWAMP Group (1985): The Sea Wave Modelling Project (SWAMP). Part 1: Principal results and Conclusions. In Ocean Wave Modelling, Plenum Press, New York and London, pp 256.

WAMDI Group (1988): A third generation ocean wave prediction model. J.Phys.Oean., 18, 1775-1810.

Weber S., H. von Storch, P. Viterbo and L. Zambresky (1991): Coupling an ocean wave model to an atmospheric general circulation model, submitted.

Zambresky, L. (1989): A verification study of the global WAM model December 1987 - November 1988.. ECMWF Technical Report No. 63. Reading, ECMWF, 86 pp.

APPENDIX A1

Wave Model Job Stream at ECMWF

APPENDIX A1: THE WAVE MODEL JOB STREAM AT ECMWF

1. INTRODUCTION

Since January 1st 1992 Cycle 4 of the WAM-WAVE-MODEL has been running quasi-operationally at ECMWF. This paper gives an overview of all jobs, their aims and dependencies, and over all input/output files, their names, locations and contents.

Presently all jobs are running on the Cray YMP under control of the emos-supervisor. All jobs and executable programmes are stored in directories on the cray disks related to emos and backed up on the ecfile system on the IBM related to emos, too. The FORTRAN source codes are on NOS/VE in the catalog ECMWF.NAB.WAMMODEL.OPER_YMP_NOVEMBER91.SET_UP. In addition this catalog includes all jobs passed to operations and a number of diagnostic programmes (see Appendix D.). 'Real time' processing of the buoy data, the ERS-1 RADAR ALTIMETER DATA and the ERS-1 AMI WAVE DATA is carried out within the job sequence.

2. THE JOBS

Currently there are five jobs. They are stored on a CRAY disk at the directory: /tmp/emos_sms/oo/owam

JOB NAME	NQS return files	auxiliary log files
1. oowam0.job	oowam0	
2. oowam1.job	oowam1	oowam1.log
3. oowam2.job	oowam2	
4. oowam3.job	oowam3	oowam3.log
5. oowam4.job	oowam4	oowam4.log

The NQS return files of these requests and the auxiliary log files are redirected to the CRAY directory: /tmp/emos_sms/log/oo/owam

In cases 1. and 3. the standard error output is directed to the standard output destination. In the other cases most of the programme output is written to the corresponding .log file.

The first job submitted by the supervisor is oowam0.job. If this job finishes successfully the job oowam1.job is submitted and then the jobs oowam2.job, oowam3.job and oowam4.job together. If any of these jobs finishes unsuccessfully, the supervisor submits the same job again. If it fails a second time the supervisor will generate an error message and the whole sequence will stop until the error is sorted out by hand. The supervisor will continue working afterwards.

2.1 oowam0.job

Since the model is operationally running, this job loses its purpose because all the duties are now shifted to the supervisor. So this job is to be seen as an historical relic from former times. It generates a file named DATE containing the emos-variables $YEAR, $MONTH and $DAY. Then a modified source of the programme CONTROL is compiled, loaded and executed. The programme CONTROL is designed to update the WAMINFO file and to allocate the next job which is to be submitted with respect to the status of the WAMINFO file.

This job is still necessary because the model and other pre- and postprocessing programmes need the correct information (at least the begin date time) from the WAMINFO file.

2.2 oowam1.job

This job executes the preprocessing programmes "preuwab" and "getinpb" and the wave model ("wavemodelb").

"preuwab" converts the locations of the AMI WAVE SPECTRA into block numbers and block indices. This list is temporarily saved on disk with the name COLYYMMDDhhmm. The wave model reads this list and writes out WAM wave spectra at these locations. These spectra are than saved into ecfile. The naming convention for the files is COSYYMMDDhhmm00. COS and COL files are saved at the ecfile node /sth/cos/uwaers1.

"preuwab" needs as input the WAMINFO file and the grid organization as stored in the file GRIDGLOU. As data input it needs the AMI WAVE DATA, stored in files with the naming convention UWAXyymmddohh at the ecfile node /oparch/ers1.

"getinpb" writes the MARS input cards and needs the WAMINFO file for the correct date/time group. The following mars request will result in a file named fort.63 containing all necessary analysis and forecast wind fields for the next wave model run.

"wavemodelb" needs as input, besides the constant user input on unit 5, the WAMINFO file and the files GRIDGLOU and UBUFGLOU. The restart files BLSPANAL, SLATANAL and LAWIANAL are fetched during the model run from the ecfile node /waj/cos/wamoper. While running, the model replaces the restart files BSLPANAL, SLATANAL, LAWIANAL, BLSPFORC, SLATFORC, LAWIFORC and the updated WAMINFO file, and it will save the output files MAP and OUT for the analysis period and for the forecast period. All these files are saved to the ecfile node /waj/cos/wamoper. Beside this the WAMIFO file is

copied to the CRAY directory /tmp/emos_oo/wamoper to enable a faster access next time it is needed. Furthermore the files UBUFGLOU and GRIDGLOU and all executable programmes are stored in this CRAY directory.

2.3 oowam2.job

This job performs the model postprocessing. The programme "postprob" plots the wind and wave field and archives the integrated model fields (MAP files) into the mars archive. In addition it will update a monthly climatology file. The naming convention for these files is MONYY and they are saved at the ecfile node /waj/cos/wamoper/climate. "postprob" is also driven by the WAMINFO file.

2.4 oowam3.job

This job generates monthly collocation files of model values and buoy data. For this purpose there are three jobs executed after each other: "cremadib", "dcdbudatab" and "extractb".

"cremadib" uses the begin date time of the WAMINFO file to generate mars input cards in order to extract the buoy data out of the mars archives for the last analysis period of the model. The mars request will result in two target files named FIRSTDAY and SECONDDAY. The contents of these two files are packed into FM 94 BUFR and there is more information retrieved by the mars request then wanted.

Therefore "dcdbudatab" is executed to decode the data and to generate unformatted written files with the information needed. The result file is named BUO and kept temporarily on the working directory.

The last programme in this sequence, "extractb", collocates the buoy and WAM-Model data. The collocation files contain data of a period of one month. That means that "extractb" is extending the current file by the new data each time running until a new month is reached. The updated file is saved at the ecfile node /waj/cos/wamoper/buoy. "extractb" is also reading the WAMINFO file in order to set the correct date for the collocation file and to check the length of the last analysis period.

2.5 oowam4.job

The main purpose of this job is to do collocation files of ERS-1 RADAR ALTIMETER DATA and WAM-Model data (SWH and wind speed). One main programme, named "uraers1b", is executed within this job. This programme calls subroutines to decode the ERS-1 data, to do a quality control on these data, to do the collocation files and to plot these information on A3 maps. Again, "uraers1b" is driven by the WAMINFO file to get the begin date/time of the last analysis period, expecting it was of 24 hours length. The quality control requires a land-see-mask which is stored at the ecfile node/sth/cos/uraers1. The file is

named LAND_SEA. The ERS-1 data are accessible from files named URAXYYMMDDohh at the ecfile node /oparch/ers1. The generated collocation files are saved at the ecfile node /sth/cos/uraers1 and named URAMYYMMDDohh. In addition, the quality control on the satellite data will result in separate files, the so called "flagged files" named URAFYYMMDDohh and saved at the same ecfile node. Furthermore the quality control serves as a pre-processing routine with respect to the collocation routine. For this purpose it generates files of averaged ERS-1 data. These files, named URAAYYMMDDohh and kept temporarily on the working directory, contain the data to be collocated with the in time and space interpolated WAM-Model values. Presently all above mentioned data files of this job contain data on a six hourly basis.

3. Monthly postprocessing jobs

These jobs are intended to examine the monthly files /waj/cos/wamoper/climate/MONYY and /waj/cos/wamoper/buoy/cbmMONYY. Currently, these programmes are running in batch-job-mode on the CRAY submitted from the CYBER. Therefore, the source codes are embedded in JCL-files located on NOS/VE at catalog :ecmwf.nab.wammodel.oper_ymp_november91.month_jobs.

3.1 CLIMATE_FILE_OUTPUT

The programme "CLIOUT" postprocesses the wave model climate file, which is generated by "postprob". It makes global plots of mean and maximum wave height and wind speeds at 10 m and generates some statistics. Additionally, the plotted fields are printed. The programme expects the climate file on the working directory named "CLI". Therefore, the wanted climate file is to be retrieved out of the ecfile system before running the programme. The following may serve as an example:

' ecfile -p /waj/cos/wamoper/climate/dec91 -tUT -enG get CLI ' No further files are needed. The printed fields are included in the NQS-return-files.

3.2 PLOT_BUOY_COLLOCATION_FILE

The programme "PLCOL" postprocesses the result files of "oowam3.job". It makes plots of time-series including some statistics and expects the input file on the working directory named "CBM". Therefore, the wanted collocation file is to be retrieved out of the ecfile system before running the programme like:

' ecfile -p /waj/cos/wamoper/BUOY/CBMDEC91 -tUT-eNG get CBM '

Each plot is a monthly time series at one buoy location. The list of buoys to be evaluated are given by the user and read in on unit 5. The following time series are plotted:

1. MODEL AND BUOY WAVE HEIGHT
2. MODEL AND BUOY WIND SPEED
3. MODEL AND BUOY WIND DIRECTION
4. AIR-SEA TEMP DIFFERENCE OBSERVED BY BUOY

The following wind and wave statistics are included:

1. MODEL MEAN AND STANDARD DEVIATION
2. OBSERVED MEAN AND STANDARD DEVIATION
3. SLOPE AND INTERCEPT OF LEAST SQUARES FIT
4. ROOT-MEAN-SQUARE ERROR
5. CORRELATION COEFFICIENT
6. SCATTER INDEX

3.3 PPRINT_BUOY_LIST_COLLOCATION_FILE

The programme "PBLIST" postprocesses the result files of "oowam3.job". It prints a list of buoys which are registered in the collocation files and expects the input file on the working directory named "CBM". Therefore, the wanted collocation file is to be retrieved out of the ecfile system before running the programme like:

' ecfile -p /waj/cos/wamoper/BUOY/CBMDEC91 -tUT-eNG get CBM '

3.4 PR_BUOY_STATS

The programme "PBLIST" postprocesses the result files of "oowam3.job". It prints statistics of wave heights and wind speeds from the collocation files and expects the input file on the working directory named "CBM". Therefore, the wanted collocation file is to be retrieved out of the ecfile system before running the programme like:

' ecfile -p /waj/cos/wamoper/BUOY/CBMDEC91 -tUT-eNG get CBM '

The monthly summary statistics are printed separately for one buoy location. The list of buoys to be evaluated are given by the user and read in on unit 5.

3. GETINPT_TO_YMP_AND_ECFILE
4. WAMODEL_TO_YMP_AND_ECFILE
5. POSTPRO_TO_YMP_AND_ECFILE
6. - 8. COLLOCATION_TO_YMP_AND_ECFILE
9. URAERS1_TO_YMP_AND_ECFILE

5.3 Dependencies between programmes and IO used variables

$ECPATH=/waj/cos/wamoper

$YMPPATH=/tmp/emos_oo/wamoper

oowam0.job

($TMPDIR/DATE) →
$YMPPATH/waminfo → CONTROL.f → $ECPATH/waminfo
→ $YMPPATH/waminfo

oowam1.job

$YMPPATH/waminfo →
$YMPPATH/gridglou →
/oparch/ers1/uwaxYYMMDDohh →

preuwab

→ /sth/cos/uwaers1/colYYMMDDhhmm00
→ ($TMPDIR/colYYMMDDhhmm)

$YMPPATH/waminfo →

getinpb

→ ($TMPDIR/fort.22) →

mars

→ ($TMPDIR/fort.63) →

generates the required windfields on the file "fort.63". The start files are saved at the ecfile node /waj/cos/wamoper as given with the user input. Additionally, "PRESET" needs as input the general grid information and model constants from the file "GRIDGLOU".

4.4 WAMIFO_TO_ECFILE

This job transfers the WAMINFO file to ecfile at node /waj/cos/wamoper.

5.1 List of used libraries

No.	name	location on CRAY disk	backup location (ecfile)
1.	wamcrlib	/ec/waj	/waj/cos/wamoper
2.	ERSLIB	/ec/waj	/waj/cos/wamoper
3.	BUFR5.a	/tmp/sth	/sth/cos/libs
4.	$EMOSLIB	/usr/local/lib	irrelevant
5.	$ECLIB	/usr/local/lib	irrelevant
6.	$MAGLIB	/usr/local/lib	irrelevant

5.2 List of used programmes

No.	name	used in job No.	required libraries
1.	CONTROL.f	1.	1.
2.	preuwab	2.	1. to 5.
3.	getinpb	2.	1.
4.	wamodelb	2.	1., 4. and 5.
5.	postprob	3.	1. and 4. to 6.
6.	cremadib	4.	1.
7.	dcdbudata	4.	1. to 5.
8.	extractb	4.	1. 3. to 5.
9.	uraers1b	5.	1. to 6.

location on CRAY disk backup location (ecfile)

1. included within oowam0.job none

2. - 9. /tmp/emos_oo/wamoper /waj/cos/wamoper

location of source codes on NOS/VE:

CATALOG :ecmwf.nab.wammodel.oper_ymp_november91.set_up

2. PREUWA_TO_YMP_AND_ECFILE

3. GETINPT_TO_YMP_AND_ECFILE
4. WAMODEL_TO_YMP_AND_ECFILE
5. POSTPRO_TO_YMP_AND_ECFILE
6. - 8. COLLOCATION_TO_YMP_AND_ECFILE
9. URAERS1_TO_YMP_AND_ECFILE

5.3 Dependencies between programmes and IO used variables

$ECPATH=/waj/cos/wamoper

$YMPPATH=/tmp/emos_oo/wamoper

oowam0.job

($TMPDIR/DATE) →
$YMPPATH/waminfo → CONTROL.f → $ECPATH/waminfo
→ $YMPPATH/waminfo

oowam1.job

$YMPPATH/waminfo →
$YMPPATH/gridglou →
/oparch/ers1/uwaxYYMMDDohh →

preuwab

→ /sth/cos/uwaers1/colYYMMDDhhmm00
→ ($TMPDIR/colYYMMDDhhmm)

$YMPPATH/waminfo →

getinpb

→ ($TMPDIR/fort.22) →

mars

→ ($TMPDIR/fort.63) →

($TMPDIR/colYYMMDDhhmm) →

$YMPPATH/waminfo →

$YMPPATH/gridglou →

$YMPPATH/ubufglou →

$ECPATH/blspanal →

$ECPATH/slatanal →

$ECPATH/lawianal →

$ECPATH/blspanal →

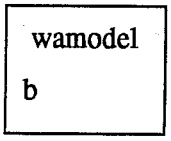

→ /sth/cos/uwaers1/colYYMMDDhhmm00

→ $ECPATH/blspanal

→ $ECPATH/slatanal

→ $ECPATH/lawianal

→ $ECPATH/blspanal

→ $ECPATH/blspforc

→ $ECPATH/mapYYMMDDhhmm0000

→ $ECPATH/outYYMMDDhhmm0000

→ $ECPATH/slatforc

→ $ECPATH/lawiforc

→ $ECPATH/blspforc

→ $ECPATH/mapYYMMDDhhmm0024

→ $ECPATH/outYYMMDDhhmm0024

→ $YMPPATH/waminfo

oowam2.job

$YMPPATH/waminfo →

$ECPATH/climat/monYY →

$ECPATH/mapYYMMDDhhmm0000 →

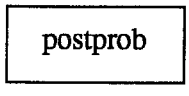

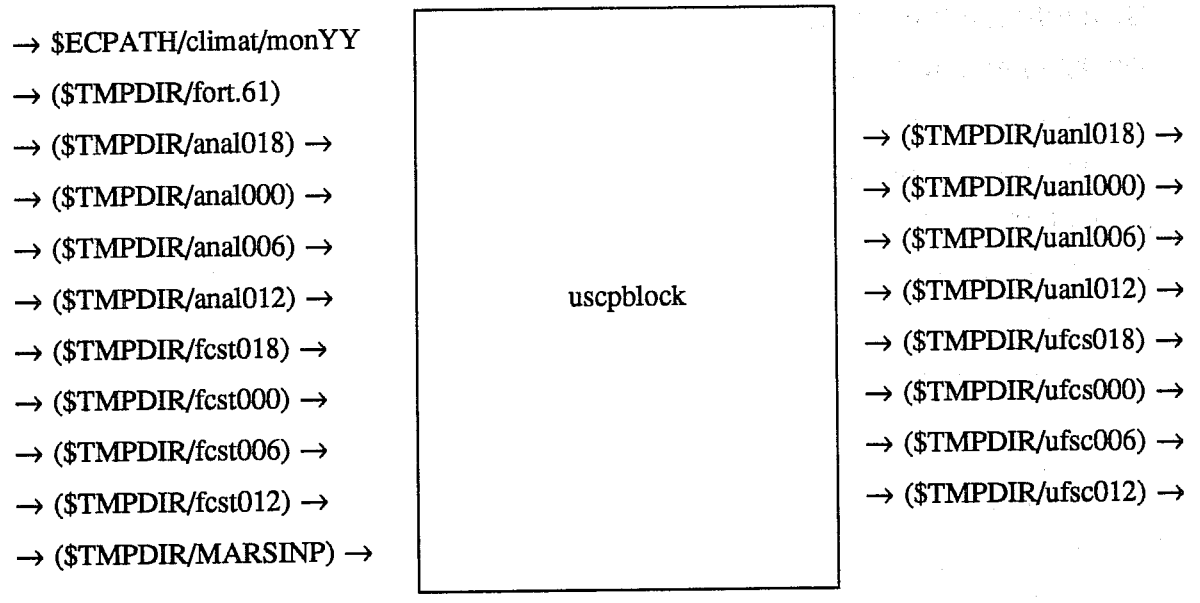

mars (archiving)

($TMPDIR/fort.61) → cp → YMPPATH/waminfo

($TMPDIR/fort.61) → ecfile → ECPATH/waminfo

oowam3.job

$YMPPATH/waminfo →

cremadib

→ ($TMPDIR/fort.22) →

mars

→ ($TMPDIR/firstday) →

→ ($TMPDIR/secondday) →

dcdbudatab

→ ($TMPDIR/BUO) →

$YMPPATH/waminfo →

$ECPATH/BUOY/CBMmonYY →

$ECPATH/mapYYMMDDhhmm0000 →

extracb

→ $ECPATH/BUOY/CBMmonYY

oowam4.job

$YMPPATH/waminfo →

/sth/cos/uraers1/land_sea →

/oparch/ers1/uraxYYMMDDohh →

$ECPATH/mapYYMMDDhhmm0000 →

preuwab

→ ($TMPDIR/fort.22) →

→ /sth/cos/uraers1/urafYYMMDDohh

→ /sth/cos/uraers1/uramYYMMDDohh

5.4 Catalog tree and catalog contents on NOS/VE related to the operationally running WAM-Model

```
ecmwf
|
|
+ → nab
|  |
:  |
   + → wammodel
   |  |
   :  |
      + → oper_ymp_november91
      |  |
      :  |
         + → diagnose
         |  |
         |  |
         |  + → blocked_map_set_up
         |
         |
         + → month_jobs
         |
         |
         + → set_up
         |  |
         |  |
         |  + → cold.start
         |
         |
         + → source_libs
```

```
CATALOG :ecmwf.nab.wammodel.oper_ymp_november91
        CATALOG: DIAGNOSE
        CATALOG: MONTH_JOBS
```

CATALOG: SET_UP

CATALOG: SOURCE_LIBS

FILE: PRINT_WAMINFO

FILE: WAM0JOB_CONTROL

FILE: WAM1JOB_WAMODEL

FILE: WAM2JOB_POSTPRO

FILE: WAM3JOB_COLOCATE_BUOY

FILE: WAM4JOB_COLOCATE_ERS1

CATALOG :ecmwf.nab.wammodel.oper_ymp_november91.diagnose

CATALOG: BLOCKED_MAP_SET_UP

FILE: AAA_READ_ME_DATA_INVENTORY

FILE: PL_1D_SPECTRA_ECFILE

FILE: PL_2D_SPECTRA_ECFILE

FILE: PL_BLOCK_ECFILE

FILE: PL_GRID_ECFILE

FILE: PL_GRID_ECFILE_DIF

FILE: PL_GRID_MARS

FILE: PL_TIMESERIE_ECFILE_OUT

FILE: PR_BLOCK_ECFILE

FILE: PR_GRID_ECFILE

FILE: PR_GRID_MARS

FILE: PR_PARAMETER_SPECTRA

FILE: PR_SPECTRA_ECFILE

FILE: PR_TIMESERIE_ECFILE_OUT

FILE: PR_TIMESERIE_MARS

CATALOG :ecmwf.nab.wammodel.oper_ymp_november91.diagnose.blocked_map_set_up

FILE: AAA_READ_ME_FIRST

FILE: PREPROC

FILE: TOPOGLO

CATALOG :ecmwf.nab.wammodel.oper_ymp_november91.month_jobs

FILE: CLIMATE_FILE_OUTPUT

FILE: PLOT_BUOY_COLOCATION_FILE

FILE: PRINT_BUOY_LIST_COLOCATION_FILE

FILE: PR_BUOY_STATS

CATALOG :ecmwf.nab.wammodel.oper_ymp_november91.set_up

CATALOG: COLD_START

FILE: COLLOCATION_TO_YMP_AND_ECFILE

FILE: ERSLIB_TO_YMP_AND_ECFILE

FILE: GETINPT_TO_YMP_AND_ECFILE

FILE: POSTPRO_TO_YMP_AND_ECFILE

FILE: PREUWA_TO_YMP_AND_ECFILE

FILE: URAERS1_TO_YMP_AND_ECFILE

FILE: WAM0JOB_TO_YMP

FILE: WAM1JOB_TO_YMP_AND_ECFILE

FILE: WAM2JOB_TO_YMP_AND_ECFILE

FILE: WAM3JOB_TO_YMP_AND_ECFILE

FILE: WAM4JOB_TO_YMP_AND_ECFILE

FILE: WAMCRLIB_TO_YMP_AND_ECFILE

FILE: WAMODEL_TO_YMP_AND_ECFILE

CATALOG :ecmwf.nab.wammodel.oper_ymp_november91.set_up.cold_start

FILE: CLIMATE_FILE_SET_UP

FILE: PREPROC

FILE: PRESET

FILE: TOPOGLO_TO_ECFILE

FILE: WAMINFO_TO_ECFILE

CATALOG :ecmwf.nab.wammodel.oper_ymp_november91.source_libs

FILE: AA_READ_ME_FIRST

FILE: EIS

FILE: PREPROC_SWAMP

FILE: PRESET_SWAMP2

FILE: WAMINFO_SWAMP

FILE: WAMODEL_LIB_3_6

FILE: WAMODEL_LIB_4

FILE: WAMODEL_LIB_4_OPER

FILE: WAMODEL_SWAMP

LIST OF ECMWF TECHNICAL REPORTS

1	A case study of a ten day forecast. September, 1976	Arpe, K., L. Bengtsson, A. Hollingsworth, and Z. Janjic
2	The effect of arithmetic precision on some meteorological integrations. December, 1976	Baede, A.P.M., D. Dent, and A. Hollingsworth
3	Mixed-radix Fourier transforms without reordering. February, 1977	Temperton, C.
4	A model for medium range weather forecasts - adiabatic formulation. March, 1977	Burridge, D.M., and J. Haseler
5	A study of some parameterisations of sub-grid processes in a baroclinic wave in a two dimensional model. July, 1977	Hollingsworth, A.
6	The ECMWF analysis and data assimilation scheme: analysis of mass and wind field. December, 1977	Lorenc, I. Rutherford and G. Larsen
7	A ten-day high-resolution non-adiabatic spectral integration; a comparative study. October, 1977	Baede, A.P.M., and A.W. Hansen
8	On the asymptotic behaviour of simple stochastic-dynamic systems. November, 1977	Wiin-Nielsen, A.
9	On balance requirements as initial conditions. October, 1978	Wiin-Nielsen, A.
10	ECMWF model parameterisation of sub-grid scale processes. January, 1979	Tiedtke, M., J.-F. Geleyn, A. Hollingsworth, and J.-F. Louis
11	Normal mode initialization for a multi-level grid-point model. April, 1979	Temperton, C., and D.L. Williamson
12	Data assimilation experiments. October, 1978	Seaman, R.
13	Comparison of medium range forecasts made with two parameterisation schemes. - , 1978	Hollingsworth, A., K. Arpe, M. Tiedke, M. Capaldo, H. Savijarvi, O. Akesson, and J.A. Woods
14	On initial conditions for non-hydrostatic models. November, 1978	Wiin-Nielsen, A.C.
15	Adiabatic formulation and organization of ECMWF's spectral model. -, 1979	Baede, A.P.M., M. Jarraud, and U. Cubasch
16	Model studies of a developing boundary layer over the ocean. November, 1979	Økland, H.
17	The response of a global barotropic model to forcing by large scale orography. January, 1980	Quiby, J.
18	Confidence limits for verification and energetic studies. May, 1980	Arpe, K.

19	A low order barotropic model on the sphere with orographic and newtonian forcing. July, 1980	Kallen, E.
20	A review of the normal mode initialization method. August, 1980	Du Xing-yuan
21	The adjoint equation technique applied to meteorological problems. September, 1980	Kontarev, G.
22	The use of empirical methods for mesoscale pressure forecasts. November, 1980	Bergthorsson, P.
23	Comparison of medium range weather forecasts made with models using spectral or finite difference techniques in the horizontal. February, 1981	Jarraud, M., C. Girard, and U. Cubasch
24	On the average errors of an ensemble of forecasts. February, 1981	Derome, J.
25	On the atmospheric factors affecting the Levantine Sea. May, 1981	Ozsoy, E.
26	Tropical influences on stationary wave motion in middle and high latitudes. August, 1981	Simmons, A.J.
27	The energy budgets in North America, North Atlantic and Europe based on ECMWF analysis and forecasts. November, 1981	Sävijärvi, H.
28	An energy and angular momentum conserving finite-difference scheme, hybrid coordinates and medium range weather forecasts. November, 1981	Simmons, A.J., and R. Strufing
29	Orographic influences on Mediterranean lee cyclogenesis and European blocking in a global numerical model. February, 1982	Tibaldi, S. and A. Buzzi
30	Review and re-assessment of ECNET - A private network with open architecture. May, 1982	Haag, A., Königshofer, F. and P. Quoilin
31	An investigation of the impact at middle and high latitudes of tropical forecast errors. August, 1982	Haseler, J.
32	Short and medium range forecast differences between a spectral and grid point model. An extensive quasi-operational comparison. August, 1982	Girard, C. and M. Jarraud
33	Numerical simulations of a case of blocking: The effects of orography and land-sea contrast. September, 1982	Ji, L.R., and S. Tibaldi
34	The impact of cloud track wind data on global analyses and medium range forecasts. December, 1982	Källberg, P., S. Uppala, N. Gustafsson, and J. Pailleux
35	Energy budget calculations at ECMWF. Part 1: Analyses 1980-81. December, 1982	Oriol, E.

36	Operational verification of ECMWF forecast fields and results for 1980-1981. February, 1983	Nieminen, R.
37	High resolution experiments with the ECMWF model: a case study. September, 1983	Dell'Osso, L.
38	The response of the ECMWF global model to the El-Niño anomaly in extended range prediction experiments. September, 1983	Cubasch, U.
39	On the parameterisation of vertical diffusion in large-scale atmospheric models. December, 1983	Manton, M.J.
40	Spectral characteristics of the ECMWF objective analysis system. December, 1983	Daley, R.
41	Systematic errors in the baroclinic waves of the ECMWF. February, 1984	Klinker, E., and M. Capaldo
42	On long stationary and transient atmospheric waves. August, 1984	Wiin-Nielsen, A.C.
43	A new convective adjustment. October, 1984	Betts, A.K., and M.J. Miller
44	Numerical experiments on the simulation of the 1979 Asian summer monsoon. October, 1984	Mohanty, U.C., R.P. Pearce and M. Tiedtke
45	The effect of mechanical forcing on the formation of a mesoscale vortex. October, 1984	Guo-xiong Wu and Shou-jun Chen
46	Cloud prediction in the ECMWF model. January, 1985	Slingo, J., and B. Ritter
47	Impact of aircraft wind data on ECMWF analyses and forecasts during the FGGE period, 8-19 November. March 1985	Baede, A.P.M., P. Kållberg, and S. Uppala
48	A numerical case study of East Asian coastal cyclogenesis. May 1985	Chen, Shou-jun and L. Dell'Osso
49	A study of the predictability of the ECMWF operational forecast model in the tropics. September 1985	Kanamitsu, M.
50	On the development of orographic. June 1985	Radinovic, D.
51	Climatology and systematic error of rainfall forecasts at ECMWF. October 1985	Molteni, F., and S. Tibaldi
52	Impact of mofified physical processes on the tropical simulation in the ECMWF model. October 1985	Mohanty, U.C., J.M. Slingo and M. Tiedtke
53	The performance and systematic errors of the ECMWF tropical forecasts (1982-1984). November 1985	Heckley, W.A.

54	Finite element schemes for the vertical discretization of the ECMWF forecast model using linear elements. January 1986	Burridge, D.M., J. Steppeler, and R. Strüfing
55	Finite element schemes for the vertical discretization of the ECMWF forecast model using quadratic and cubic elements. February 1986	Steppeler, J.
56	Sensitivity of medium-range weather forecasts to the use of an envelope orography. September 1986	Jarraud, M., A.J. Simmons and M. Kanamitsu
57	Zonal diagnostics of the ECMWF operational analyses and forecasts. October 1986	Branković, Č.
58	An evaluation of the performance of the ECMWF operational forecasting system in analysing and forecasting tropical easterly disturbances. Part 1: Synoptic investigation. September 1986	Reed, R.J., A. Hollingsworth, W.A. Heckley and F. Delsol
59	Diabatic nonlinear normal mode initialisation for a spectral model with a hybrid vertical coordinate. January 1987	Wergen, W.
60	An evaluation of the performance of the ECMWF operational forecasting system in analysing and forecasting tropical easterly wave disturbances. Part 2: Spectral investigation. January 1987	Reed, R.J., E. Klinker and A. Hollingsworth
61	Empirical orthogonal function analysis in the zonal and eddy components of 500 mb height fields in the Northern extratropics. January 1987	Molteni, F.
62	Atmospheric effective angular momentum functions for 1986-1987. February 1989	Sakellarides, G.
63	A verification study of the global WAM model December 1987 - November 1988. May 1989	Zambresky, L.
64	Impact of a change of radiation transfer scheme in the ECMWF model. November 1989	Morcrette, J-J.
65	The ECMWF analysis-forecast system during AMEX. May 1990	Puri, K., P. Lönnberg and M. Miller
66	The calculation of geopotential and the pressure gradient in the ECMWF atmospheric model: Influence on the simulation of the polar atmosphere and on temperature analyses. July 1990	Simmons, A.J. and Chen Jiabin
67	Assimilation of altimeter data in a global third generation wave model February 1992	Lionello, P., H. Günther and P. Janssen